



## **TABLE OF CONTENTS**

	<u>Page</u>
<b>I. INTRODUCTION</b>	<b>2</b>
<b>II. PHASE I TECHNICAL OBJECTIVES</b>	<b>5</b>
<b>III. WORK PERFORMED AND RESULTS OBTAINED</b>	<b>6</b>
<b>Task 1 Preparation of Anodes, Microparticles, and Preliminary ECM of Titanium Alloys</b>	<b>8</b>
a. Materials Preparation	8
b. Voltammetry	8
c. Preliminary Experiments on Electrochemical Machining	9
<b>Task 2 Fabrication of and Performance Improvement to Cell for Electrochemical Machining</b>	<b>14</b>
a. Preliminary ECM Results in the Absence of Heterogeneous Dispersants Within the Aqueous Electrolyte	15
b. Implementation of Experimental Design for ECM in Heterogeneous Electrolytes	15
<b>Task 3 Electrochemical Machining of Small Diameter Holes in Titanium Alloy Coupons</b>	<b>45</b>
<b>IV. SUMMARY OF PHASE I RESULTS</b>	<b>45</b>
<b>V. ESTIMATE OF TECHNICAL FEASIBILITY</b>	<b>47</b>
<b>VI. TOWARDS COMMERCIALIZATION</b>	<b>49</b>
A) Commercial Applications	49
B) Patent Status	49
C) Uniqueness of the Technology Approach	49
D) Markets	50
E) Anticipated Competition	50
F) Competitive Advantages	51
G) Towards Commercial Production	51
H) Marketing Plan	52
<b>VII. REFERENCES</b>	<b>53</b>

## LIST OF FIGURES

	<u>Page</u>
Figure 1. Schematic of empirical processes occurring during the electrochemical machining of titanium alloys when using dispersions of electronically conducting particles in ionically conducting aqueous electrolyte.	4
Figure 2. Schematic comparison of electrochemical machining using A) a homogeneous exclusively ionic conducting aqueous electrolyte and B) a heterogeneous mixed ionic and electronic conducting aqueous electrolyte, for the machining of titanium alloys used in Navy aircraft engines. Higher rates, precision, and lower effective ECM operating power requirements have were found using the latter heterogeneous electrolyte strategy where electronically conducting particles facilitate extending the cathode into close proximity to the titanium alloy anode workpiece.	7
Figure 3. Electrochemical cell for preliminary electrochemical machining experiments on titanium alloy substrates.	9
Figure 4. Cyclic voltammograms for A) Ti (99%), B) Ti 6-4, C) Ti 6242, and D) Ti <sub>3</sub> Al, in 3.15M NaBr/1.26M NaNO <sub>3</sub> , as a function of XC72R volume fraction.	10
Figure 5. Plot of material removal efficiency and cut dispersion for the ECM of titanium in 1M NaCl as a function of volume percentage graphitized carbon (XC72R) introduced into the heterogeneous electrolyte.	11
Figure 6. Photographs of Ti coupons subjected to electrodisolution with conical tip graphite cathode in 1M NaCl as a function of XC72R volume concentration. A) 0%, B) 15%, C) 25%, and D) 45% XC72R.	13
Figure 7. Schematic of bench scale apparatus designed and fabricated during Phase I for electrochemically drilling holes into titanium and titanium alloys.	14
Figure 8. Photograph of prototype ECM lathe fabricated at Eltron incorporating a stepper motor driven translational stage.	16
Figure 9. Photograph of overall ECM lathe assembly used during performance of Phase I for the machining of titanium alloys.	16

## LIST OF FIGURES, Continued

	<u>Page</u>
Figure 10. Normal probability plot for multiple regression coefficients obtained from Plackett-Burman experiments for A) material removal and B) cut depth.	26
Figure 11. Material removal, cut dispersion, and cell voltage data for the ECM of Ti using untreated XC72R particles. Aqueous electrolyte: 3.15M NaBr/1.26M NaNO <sub>3</sub> .	30
Figure 12. Photographs of Ti coupons subjected to electrodisolution in 3.15M NaBr/1.26M NaNO <sub>3</sub> with A) 0%, B) 15%, C) 25%, D) 35%, E) 55%, and F) 65% untreated XC72R (by volume). Uniform magnification was used for all photographs.	31
Figure 13. Material removal, cut dispersion, and cell voltage data for the ECM of Ti using heat treated (at 500°C) XC72R particles. Aqueous electrolyte: 3.15M NaBr/1.26M NaNO <sub>3</sub> .	32
Figure 14. Photographs of Ti coupons subjected to electrodisolution in 3.15M NaBr/1.26M NaNO <sub>3</sub> with A) 0%, B) 15%, C) 25%, D) 35%, E) 55%, and F) 65%vol% XC72R (heat treated in air at 500°C).	33
Figure 15. Material removal, cut dispersion, and cell voltage data for the ECM of Ti using Na zeolite-Y particles. Aqueous electrolyte: 3.15M NaBr/1.26M NaNO <sub>3</sub> .	34
Figure 16. Material removal, cut dispersion, and cell voltage data for the ECM of Ti using MnO <sub>2</sub> particles. Aqueous electrolyte: 3.15M NaBr/1.26M NaNO <sub>3</sub> .	35
Figure 17. Material removal, cut dispersion, and cell voltage data for the ECM of Ti 6-4 using Na zeolite-Y particles. Aqueous electrolyte: 3.15M NaBr/1.26M NaNO <sub>3</sub> .	36
Figure 18. Material removal, cut dispersion, and cell voltage data for the ECM of Ti 6-4 using heat treated XC72R (at 500°C) particles. Aqueous electrolyte: 3.15M NaBr/1.26M NaNO <sub>3</sub> .	37
Figure 19. Material removal, cut dispersion, and cell voltage data for the ECM of Ti 6-4 using untreated XC72R particles. Aqueous electrolyte: 3.15M NaBr/1.26M NaNO <sub>3</sub> .	39

## LIST OF FIGURES, Continued

	<u>Page</u>
Figure 20. Material removal, cut dispersion, and cell voltage data for the ECM of Ti 6-4 using MnO <sub>2</sub> particles. Aqueous electrolyte: 3.15M NaBr/1.26M NaNO <sub>3</sub> .	40
Figure 21. Material removal, cut dispersion, and cell voltage data for the ECM of Ti 6242 using MnO <sub>2</sub> particles. Aqueous electrolyte: 3.15M NaBr/1.26M NaNO <sub>3</sub> .	41
Figure 22. Material removal, cut dispersion, and cell voltage data for the ECM of Ti 6242 using heat treated (at 500°C) XC72R particles. Aqueous electrolyte: 3.15M NaBr/1.26M NaNO <sub>3</sub> .	42
Figure 23. Material removal, cut dispersion, and cell voltage data for the ECM of Ti 6242 using untreated XC72R particles. Aqueous electrolyte: 3.15M NaBr/1.26M NaNO <sub>3</sub> .	43
Figure 24. Material removal, cut dispersion, and cell voltage data for the ECM of Ti 6242 using Na zeolite-Y particles. Aqueous electrolyte: 3.15M NaBr/1.26M NaNO <sub>3</sub> .	44
Figure 25. Schematic of production hardware to evolve in the course of this program for the ECM of titanium alloys into turbine blisks for Navy aircraft.	48
Figure 26. Schematic of overall process for the processing and recycling of heterogeneous electrolytes used in the ECM of titanium alloys.	48

## **LIST OF TABLES**

	<u>Page</u>
<b>Table 1. Systematic Experimental Results Obtained on Selected Titanium Alloys Using Electrochemical Half-Cell</b>	<b>12</b>
<b>Table 2. Preliminary Experimental Results Obtained on Selected Titanium Alloys Using a One-Axis ECM Lathe In the Absence of Electronically Conducting Particulates</b>	<b>17</b>
<b>Table 3. Plackett-Burman Experimental Design for ECM of Titanium Alloys</b>	<b>20</b>
<b>Table 4. Results Obtained from Experiments Conducted According to Plackett-Burman Design To Determine Influence of Heterogeneous Electrolyte on ECM</b>	<b>21</b>
<b>Table 5. z-Transformed Data from Experiments Performed According to Plackett-Burman Design</b>	<b>23</b>
<b>Table 6. Multiple Regression Correlation Coefficients for Fits to Plackett Burman Data</b>	<b>23</b>
<b>Table 7. Dimensionless Multiple Regression Coefficients for Fit of Experimental Results Obtained from Plackett-Burman Design to Experimental Variables</b>	<b>25</b>

## I. INTRODUCTION

This investigation addressed the exploratory development of novel ElectroChemical Machining (ECM) technology for the shaping of titanium alloy components used in Navy aircraft gas turbine engines. Emphasis in this program was on the processing of respective materials Ti, Ti<sub>3</sub>Al, Ti 6242 (86% Ti, 6% Al, 2% Mo, 4% Zr, and 2% Sn) and Ti 6-4 (90% Ti, 6% Al and 4% V). The overall approach relied upon application of heterogeneous aqueous electrolytes as a strategy for enhancing both the rate and precision of ECM technologies for the subject application, while simultaneously lowering electrical energy power requirements for this process. It was anticipated that the presence of rationally selected electronically conducting particles suspended within the aqueous electrolyte would lead to lowering i) the incidence of interelectrode sparking, ii) Joule heating, iii) cathode polarization, while iv) enhancing dimension control for the titanium alloy anode workpiece being subjected to ECM. Electronically conducting particles incorporated within aqueous electrolytes evaluated in this program included, partially graphitized carbon (XC72R, Cabot Corporation), manganese dioxide (MnO<sub>2</sub>), titanium, and silver. The utility of ionically conducting particles of sodium zeolite-Y within the aqueous electrolyte, was also evaluated for enhancing ECM. While emphasis during Phase I program was on applying this approach to aqueous electrolytes, experimental evidence supported that this general approach would also be applicable to non-aqueous electrolytes including molten salts.

The employment of ECM<sup>1-5</sup> in the manufacture of high performance aircraft engine components has arisen because of the need to identify effective machining techniques for material removal, shaping, and finishing of hard, tough, energy absorbing components encountered in such applications. The need for rapid processing of titanium alloys into turbine blades with airfoils possessing curved surfaces gives rise to the need for complementary technologies which require only a minimum in translational motion to achieve the desired geometry while simultaneously allowing for rapid material removal, adequate dimensional control, and achieving a high quality surface finish. In comparison conventional machining methods, which require direct mechanical contact between the tool and workpiece to facilitate boring, milling, grinding, and deburring, have proven very difficult to effectively apply for the processing of such materials. Furthermore bulk material properties of components can become adversely affected as a consequence of physical stresses associated with conventional mechanical machining techniques.

In contrast, ECM technology permits rapid metal removal to be achieved with drastically reduced tool (cathode) wear, thereby allowing high dimensional control to be maintained for extended times together with facilitating high quality surface finishes. Both material removal and surface finish processing steps can also be achieved using a single ECM feed.

The anticipated employment of advanced materials typified by intermetallics (iron, nickel, and titanium aluminides), superalloys, and ceramics such as silicon carbide and silicon nitride<sup>6</sup> in high performance aircraft engines places additional burden upon machining technologies because of their even greater refractoriness than titanium alloys investigated in this program. Materials used in gas turbine units are typically more difficult to ECM because of their susceptibility towards formation of passive oxide films during anodic

material removal. Such films are not always uniformly removed from the metal substrate during conventional ECM. This can result in stray pitting and loss of acceptable workpiece dimensional control. Material removal during conventional ECM can exhibit poor current efficiencies unless the process proceeds in aggressive aqueous halide electrolytes. Fluoride and chloride based aqueous electrolytes can however lead to wild cutting (i.e. stray electrolysis and poor control of workpiece dimensions), yet it is this ability of such media to dissolve passive oxide films that make them particularly useful for this technology application.

Prior to the inception of work at Eltron ECM was a process which proceeded with very high ohmic losses, as a consequence of low ionic conductivity by the liquid electrolyte. This can result in: 1) the region between the anode workpiece and cathode dissipating a significant fraction of electrical energy as heat and consequently requiring rapid electrolyte flow to achieve thermal management and 2) the presence of non-uniform electrolyte heating resulting in nonuniform current density, as a consequence of differences in ionic conductivity within the interelectrode spacing between the workpiece (anode) and cathode. This can, for example, lead to a tapering of holes drilled by ECM and thereby compromise achievable geometric tolerances.

Such ECM performance restrictions discussed above were addressed in this program by the incorporation of electronically conducting particulate dispersions within the aqueous electrolyte. This served to effectively extend the cathode, via the resulting heterogeneous electrolyte, into close proximity to the anode workpiece<sup>7,8</sup> thereby facilitating both improved dimensional control and a lower operating voltage.

The employment of particulate dispersions in ECM was suggested as a strategy by the recognition that the occurrence of a percolation threshold in systems incorporating electronically conducting particles may also give rise to oscillatory shorting between anode and cathode, thereby reducing heating problems. Also, at the typical high current densities associated with ECM, sparking was anticipated to be eliminated by the very substantial decrease in effective dielectric constant of the heterogeneous electrolyte between the cathode and anode workpiece. A schematic of phenomena occurring in the subject heterogeneous electrolytes leading to titanium anode workpiece dissolution is shown in Figure 1.

The application of heterogeneous aqueous electrolytes for promoting the ECM of titanium and titanium alloys employed in air breathing gas turbines was expected, at the inception of this program, to facilitate several favorable effects upon overall ECM performance. These may be summarized as follows:

1. At the critical concentration (i.e. where a transition between particles in an electrically noninteracting state to a state in which particles interact with each other to the point of very briefly shorting), stochastic or random shorting can result in minimizing catastrophic sparking.
2. Dispersed particles in flowing heterogeneous electrolytes can interact with the anode workpiece surface thereby locally modifying both chemical and physical properties to improve titanium alloy surface finish, preventing passive film formation, and in addition blocking surfaces external to that being subjected to ECM.



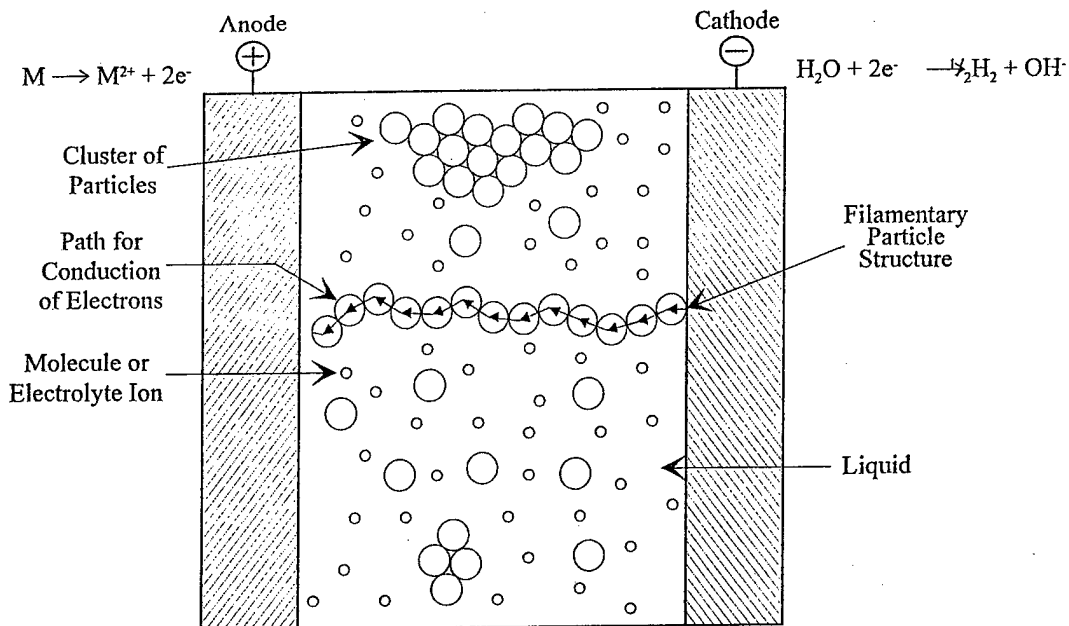


**Figure 1. Schematic of empirical processes occurring during the electrochemical machining of titanium alloys when using dispersions of electronically conducting particles in ionically conducting aqueous electrolyte.**

3. The presence of electronically conducting particles in sufficient concentrations can result in electrorheological effects which give rise to more well defined ionic migration and diffusion paths, thereby favorably influencing ECM rates and overall precision. The particles can also result in a predominance of electronic conductivity outside the cathode profile resulting in improved dimensional control.
4. At the critical concentration, the occurrence of enhanced order in the heterogeneous electrolyte can result in more uniform material removal from the workpiece region of interest as a consequence of medium ordering and better constraint of ionic conduction paths, thereby giving improved ECM dimensional control.
5. Enhanced material removal from a titanium alloy workpiece under flowing heterogeneous electrolyte conditions can result from several effects including i) the mechanical impact of particles with the titanium alloy workpiece surface, thereby facilitating reaction product removal - this in turn can increase titanium dissolution kinetics compared to that for competitive (oxygen evolution) reactions, ii) sorption of metal hydroxides, hydrous oxides, and metal oxides, originating from titanium oxidation on particles dispersed in the heterogeneous electrolyte, can also result in enhancing removal of reaction products from the anode workpiece, and iii) chemical interaction between particles and anode surface can result in the formation of chemical bonds between particles and titanium alloy anode surfaces which can weaken bonds sufficiently to facilitate improved material removal rates.
6. By effectively increasing the cathode surface area the localized rate for parasitic gas (hydrogen) evolution would be expected to decrease for a given geometric current density because of a lower effective operating overpotential, thereby contributing to improved dimensional control for the titanium alloy being subjected to ECM.

7. The subject heterogeneous electrolytes' lower interelectrode resistance, reduce the amount of Joule heating at the workpiece, thereby contributing to improved ECM dimensional control.
8. The localized concentration of dispersed particles at the titanium alloy workpiece surface subjected to ECM would be expected strongly dependent on heterogeneous electrolyte flow velocity which in turn influences the ability to both physically and chemically remove reaction products from this region.

Other than work being performed at Eltron there is no previous evidence of heterogeneous electrolytes being used to enhance the performance of titanium alloy ECM. Previous investigations have however used cathodes incorporating attached abrasive particles<sup>9</sup> for mechanically removing passivating films from the metal workpiece surface by physically moving the cathode over this region. The utility of increasing the effective cathode area with porous materials has also been discussed<sup>10</sup> and resulted, as one would expect, in lower operating overpotentials.

The use of particulate dispersions in electrochemistry has been described previously,<sup>11-14</sup> but has not been applied to ECM. The use of carbon pastes, a particulate dispersion in hydrocarbons, has been described for the analysis of solid minerals.<sup>15-18</sup> However, ECM with such heterogeneous dispersions has not been reported prior to the inception of investigations at Eltron.

As will become evident in this Final Report the application of electronically conductive particles incorporated into aqueous electrolytes was shown effective for enhancing the ECM of titanium alloys of relevance to the manufacture of air breathing gas turbine engines for Navy aircraft propulsion.

## **II. PHASE I TECHNICAL OBJECTIVES**

This program addressed applying heterogeneous aqueous electrolytes towards improving the ECM of titanium alloys employed as high temperature surfaces in Navy aircraft gas turbine engines. Experimental technical objectives were met by the introduction of dispersed suspended conductive microparticles in aqueous electrolytes of respectively NaCl, NaBr, NaBr/NaNO<sub>3</sub> mixtures, and NaNO<sub>3</sub>, for application in the ECM process. As will become evident the general approach resulted in significantly improving ECM performance for shaping titanium alloy components for the subject application compared to conventional aqueous electrolytes. This was a consequence of the heterogeneous electrolytes favorably influencing localized chemical, electrochemical, and transport phenomena at the titanium alloy workpiece during ECM.

The above overall program goal was met by addressing the following specific objectives:

- Preparing Ti, Ti<sub>3</sub>Al, Ti 6242, and Ti 6-4 coupons for ECM, by cutting, and grinding, followed by subsequent metallographic polishing.
- Conducting preliminary investigations into the electrochemical susceptibility of anode substrates (Ti, Ti<sub>3</sub>Al, Ti 6242, and Ti 6-4) to dissolution in the subject aqueous electrolytes both in the presence and absence (as a control) of heterogeneous

dispersions in an electrochemical half-cell.

- Fabricating an ECM experimental assembly incorporating a translational table to facilitate the desired orientation of cathode relative to the titanium alloy anode workpiece.
- Performing the ECM of holes in appropriately prepared titanium alloy coupons in the aqueous electrolytes NaCl, NaBr, NaBr/NaNO<sub>3</sub> mixtures, and NaNO<sub>3</sub> as a function of applied current density and voltage, anode-cathode gap, electrolyte composition both with and without a particles, and electrolyte flow rate.
- Performing a two level Plackett-Burman experimental design towards selecting preferred parameters and experimental conditions for achieving high rate precision ECM.
- Microscopically examine ECM cuts on titanium alloys to verify geometric tolerances and that desired morphological features were achieved.
- Fabricating an ECM experimental assembly based on a precision lathe to facilitate appropriate translations and rotations of tool and workpiece incorporating technology identified during this program.
- Electrochemically machining holes in titanium alloy coupons using preferred heterogeneous aqueous electrolyte compositions and experimental conditions as a function of particle concentration and type using the above ECM lathe.

Successful completion of this Phase I program resulted in determining the viability of the proposed ECM technology towards the shaping of titanium based alloys. This investigation will facilitate ready upgrading of current technology to improve performance obtain towards the ECM of titanium alloys. This will provide a significant advance in the ECM processing of titanium alloys used in Navy aircraft engines.

### **III. WORK PERFORMED AND RESULTS OBTAINED**

This program addressed the development of technology for improving the ECM of titanium alloys in novel heterogeneous aqueous electrolytes. The approach utilized suspended dispersions of conductive particles within the aqueous electrolyte to extend the cathode tool into close proximity to the titanium alloy anode workpiece being subjected to ECM. This resulted in both lowering the required operating voltage and facilitated greater precision. The intrinsic advantages of the subject heterogeneous electrolytes for ECM may be illustrated by reference to Figure 2 which schematically compares the relative effect of using homogeneous (2A) and heterogeneous (2B) aqueous electrolytes towards achieving geometric tolerance.

Voltammetry measurements on the subject titanium alloys were initially performed in the presence and absence of electronically conducting particles dispersed within selected aqueous electrolytes. Following identification of preferred electrochemical conditions for the

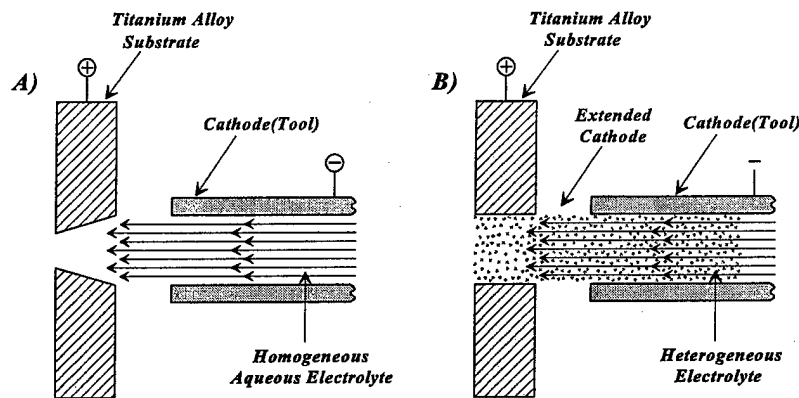


**Figure 2.** Schematic comparison of electrochemical machining using A) a homogeneous exclusively ionic conducting aqueous electrolyte and B) a heterogeneous mixed ionic and electronic conducting aqueous electrolyte, for the machining of titanium alloys used in Navy aircraft engines. Higher rates, precision, and lower effective ECM operating power requirements have been found using the latter heterogeneous electrolyte strategy where electronically conducting particles facilitate extending the cathode into close proximity to the titanium alloy anode workpiece.

processing of titanium alloys, electrochemical machining hardware was designed and incorporated into a precision lathe with automatic axial drive used to perform electrochemical machining on the subject titanium alloys. This hardware permitted continuous tool (cathode) feed towards the titanium workpiece at a controlled rate. In fully mature technology a feedback controlled tool movement based upon the titanium alloy workpiece-tool operating voltage will be incorporated.

This experimental program was performed by completing the following three tasks:

- Task 1**      **Preparation of Anodes, Microparticles, and Preliminary ECM of Titanium Alloys**
- Task 2**      **Fabrication of and Performance Improvement to Cell for Electrochemical Machining**
- Task 3**      **Electrochemical Machining of Small Diameter Holes in Titanium Alloy Coupons**

Work performed during Phase I in each of these three tasks will now be discussed.

## **Task 1      *Preparation of Anodes, Microparticles, and Preliminary ECM of Titanium Alloys***

The objective of work performed in this task was to prepare titanium and titanium alloy metal substrates for initial electrochemical machining in the presence of electronically conductive particles dispersed within aqueous electrolytes for enhancing overall ECM performance.

### **a.      Materials Preparation**

Procedures for preparing titanium alloy coupons used in performing preliminary ECM in this task involved initially cutting to the desired shape followed by sequentially polishing with 120, 360, 600 and 1200 grit SiC. Resulting titanium alloy metal specimens were then rinsed with distilled water, followed by degreasing in trichlorethylene vapor. For all samples evaluated in this program the current collection configuration to the titanium alloy coupon under test provided for both uniformity of current distribution across the anode during initial electrochemical measurements and mechanical support. Current collection wires (Ni/Cr) were attached by spot welding and isolated from the heterogeneous electrolyte by the application of Teflon heat shrink tubing.

Dispersions of electronically conducting particles in aqueous electrolyte emphasized partially graphitized carbon, (XC72R, 30nm), Na zeolite-Y ( $5\mu\text{m}$ ), and  $\text{MnO}_2$  ( $5\mu\text{m}$ ) all of which were obtained from commercial sources. We also evaluated the utility of Ag and Ti dispersions in aqueous electrolytes for this application. Difficulties however were found in satisfactorily maintaining dispersions of these latter particles in aqueous electrolyte due in part to their high density compared to the aqueous phase. For the other previously discussed particles, suspensions could be satisfactorily maintained by sparging with compressed argon. Dispersions of partially graphitized carbon required introduction of the dispersant Triton X-100 at concentrations corresponding to 3-5 drops/100ml of electrolyte.

To be now discussed is preliminary electrochemistry performed upon Ti,  $\text{Ti}_3\text{Al}$ , Ti 6242, and Ti 6-4 substrates using a conventional three electrode electrochemical cell shown in Figure 3.

### **b.      Voltammetry**

Initial electrochemical experiments consisted of performing Cyclic Voltammograms (CV's) on candidate titanium alloys in 3.15M NaBr/1.26M  $\text{NaNO}_3$  as a function of volume % partially graphitized carbon introduced, under continuous vigorous stirring. The electrolyte was selected as a presently preferred composition following conversations between Eltron and the GE Jet Engines Division. CV's for Ti (99.6%) in 3.15M NaBr/1.26M  $\text{NaNO}_3$ /XC72R are shown in Figure 4A as a function of XC72R fraction in the electrolyte. The voltammogram for carbon-free electrolyte shows that the metal oxidation wave was followed by that for oxygen evolution. Introduction of 35% XC72R into the aqueous electrolyte resulted in an almost four-fold increase in titanium oxidation current. Addition of 65vol% XC72R apparently resulted in the occurrence of fast and large amplitude oscillations or direct electronic short circuiting of sufficient duration to cause current compliance of the

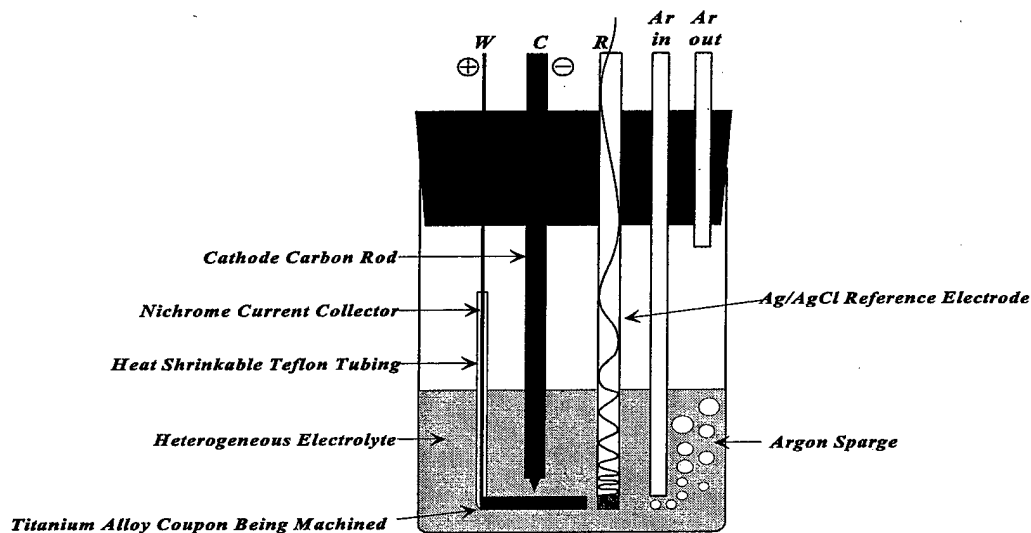


**Figure 3.** Electrochemical cell for preliminary electrochemical machining experiments on titanium alloy substrates.

instrument to be reached. In contrast to titanium metal, Ti 6-4 demonstrated decreasing oxidation current with XC72R fraction, such that a perceptible metal oxidation wave was not obtained at 65vol% XC72R.

Ti 6242, (Figure 4C) like Ti 6-4, demonstrated suppression of metal oxidation current with increased XC72R volume concentration. The suppression of oxidation current was accompanied by the appearance of a diffusion type wave on the reductive side of the voltammogram. This was probably due to either the presence of soluble oxidation reaction products in solution, or to catalytic reduction of dissolved oxygen generated during solvent breakdown. The most notable feature in Ti<sub>3</sub>Al (Figure 4D) voltammetry was the apparent increase in Ti<sub>3</sub>Al oxidation current at higher applied anodic potential and XC72R fraction.

In general, addition of XC72R partially graphitized carbon to the ionically conducting electrolyte resulted in enhanced titanium oxidation currents.

### c. Preliminary Experiments on Electrochemical Machining

Experiments were again performed using the electrochemical arrangement shown above schematically in Figure 3. The electrochemical configuration consisted of a titanium alloy anode coupon being subjected to electrochemical machining, a Ag/AgCl reference electrode in close proximity and a conically pointed carbon rod cathode. The conical point provided a uniformly graded potential to the anode surface so that the effect of a continuously variable localized current density could be observed for a given titanium metal alloy. This was of particular importance in determining the susceptibility of the titanium alloy workpiece to any stray dissolution outside the footprint of the cathode of the substrate being electrochemically machined. The electrolyte was continuously stirred.

Preferred aqueous electrolytes for promoting the electrochemical removal of a given

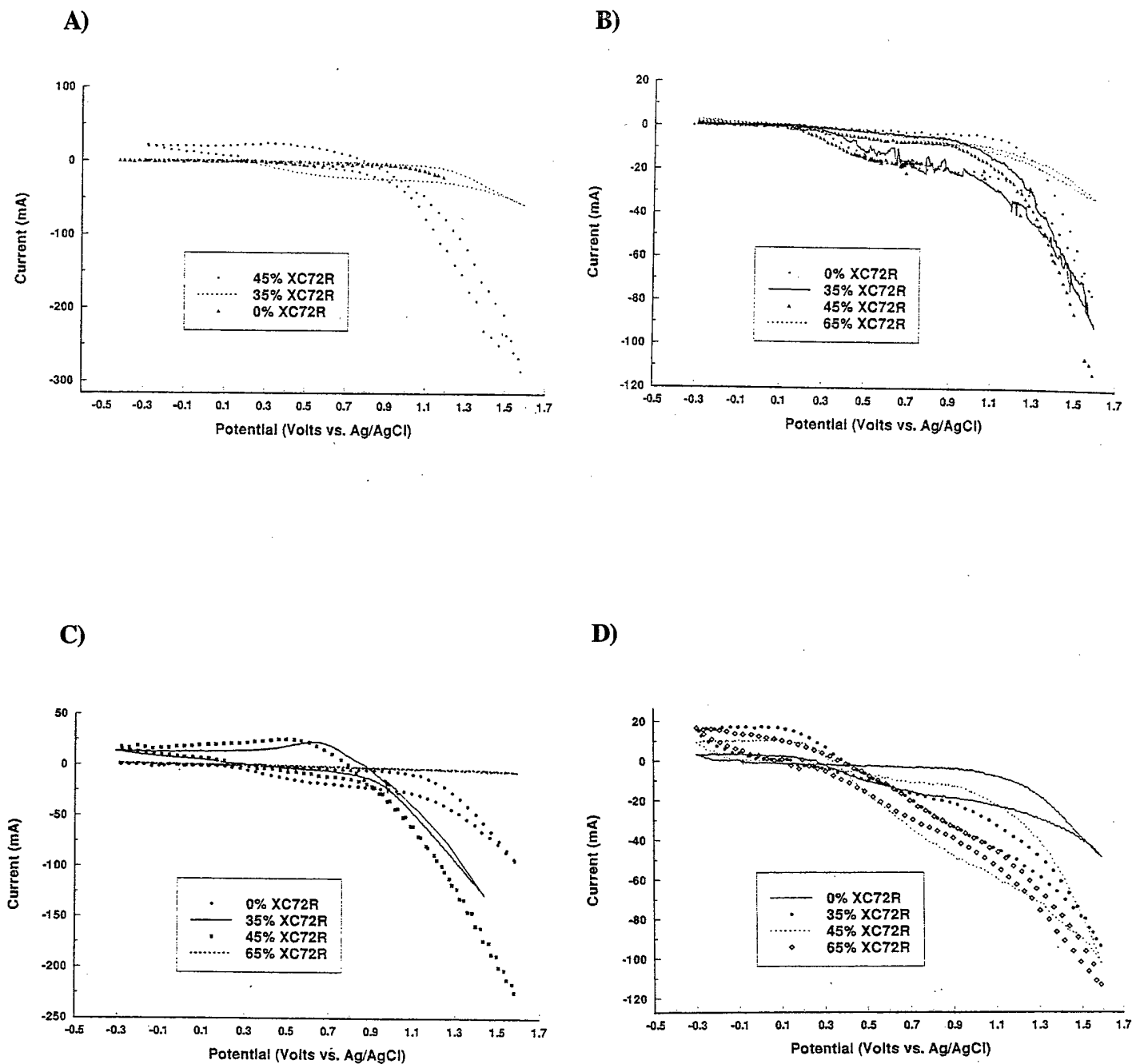


**Figure 4.** Cyclic voltammograms for A) Ti (99%), B) Ti 6-4, C) Ti 6242, and D) Ti<sub>3</sub>Al, in 3.15M NaBr/1.26M NaNO<sub>3</sub>, as a function of XC72R volume fraction.

titanium anode material were initially evaluated in this electrochemical configuration in the absence of conducting particles. Preferred aqueous electrolytes found to minimize surface passivation effects during electrochemical material removal included 3.15M NaBr/1.26M NaNO<sub>3</sub>, and 1M NaCl. Representative results for titanium oxidation efficiency and dimensional control as a function of XC72R dispersion in NaCl is shown in Figure 5. Material removal and cut dispersion (dimensional control) data are presented in Table 1. Cut dispersion was defined as the diameter of the primary anodically dissolved region (as distinguished from stray pitting). Optimum cut geometric tolerance was observed above 25vol% XC72R dispersed within the aqueous electrolyte. Photographs of titanium alloy coupons subjected to these experiments are presented in Figure 6 which illustrate features represented by the cut dispersion plot in Figure 5 - namely the tendency for cuts made with volume concentrations of greater than 25% XC72R to focus with increasing carbon concentration. In general shape resolution was improved by the addition of XC72R into the aqueous electrolyte. Cathode features were not visible in these cuts. However, cut focussing obtained with increasing carbon concentration can be regarded as improvement in lateral shape resolution.

Experimental completion of this task resulted in gaining insight into those heterogeneous electrolytes and electrochemical operating conditions leading to higher ECM rates and inhibition of stray dissolution for the subject titanium alloys using a conventional three electrode cell arrangement where the influence of flowing heterogeneous electrolyte onto the anode workpiece was absent. These findings contributed to the design, fabrication and selection of operating conditions for a prototype ECM lathe in the next task.

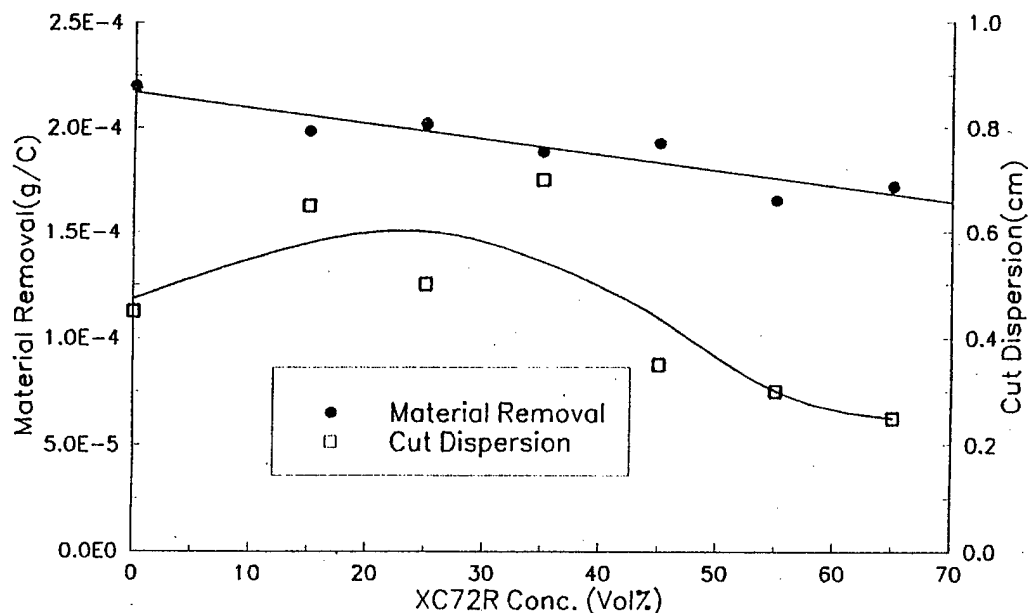


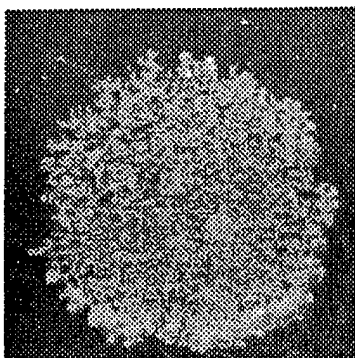
Figure 5. Plot of material removal efficiency and cut dispersion for the ECM of titanium in 1M NaCl as a function of volume percentage graphitized carbon (XC72R) introduced into the heterogeneous electrolyte.



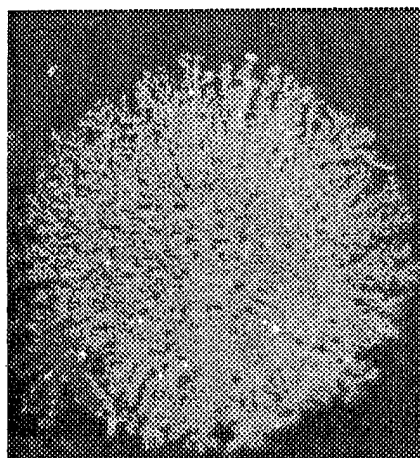
**Table 1.**  
**Systematic Experimental Results Obtained on Selected Titanium Alloys Using Electrochemical Half-Cell**

Coupon #	Material	Apparatus	Bit Type	Electrolyte Used	Coupon Weight Loss (grams)	Current Applied (mAmps)	Length of Trial (Sec)	Charge Applied (Coulombs)	Volume Electrolyte (ml.)	Material Removed per charge (grams/coulomb)	Cut Depth (mm)	Cut Diameter (mm)	Bit to Coupon	
													Distance (microns)	Bit Speed (mm/sec)
27	Titanium (99.6+ % Pure)	Beaker	Carbon Rod	1 M NaCl	0.0381	500 to 1000	300	145	60	0.0002628	0	N/A	500	N/A
28	Titanium (99.6+ % Pure)	Beaker	Carbon Rod	1 M NaCl	0.0359	900 to 1000	174	156	60	0.0002301	0	N/A	500	N/A
29	Titanium (99.6+ % Pure)	Beaker	Carbon Rod	1 M NaCl	0.0264	900 to 1000	127	120	60	0.00022	0	N/A	500	N/A
30	Titanium (99.6+ % Pure)	Beaker	Carbon Rod	65% XC72R/35% 1 M NaCl	0.0206	500 to 750	189	120	60	0.0001717	0	N/A	500	N/A
31	Titanium (99.6% Pure)	Beaker	Carbon Rod	15% XC72R/85% 1 M NaCl	0.0238	850 to 1000	123	120	60	0.0001983	0	N/A	500	N/A
32	Titanium (99.6% Pure)	Beaker	Carbon Rod	25% XC72R/75% 1 M NaCl	0.0242	800 to 1000	132	120	60	0.0002017	0	N/A	500	N/A
33	Titanium (99.6+ % Pure)	Beaker	Carbon Rod	35% XC72R/65% 1 M NaCl	0.0226	800 to 1000	132	120	60	0.0001883	0	N/A	500	N/A
34	Titanium (99.6+ % Pure)	Beaker	Carbon Rod	55% XC72R/45% 1 M NaCl	0.0198	300 to 600	255	120	60	0.000165	0	N/A	500	N/A
35	Titanium (99.6+ % Pure)	Beaker	Carbon Rod	45% XC72R/55% 1 M NaCl	0.0231	700 to 1000	141	120	60	0.0001925	0	N/A	500	N/A

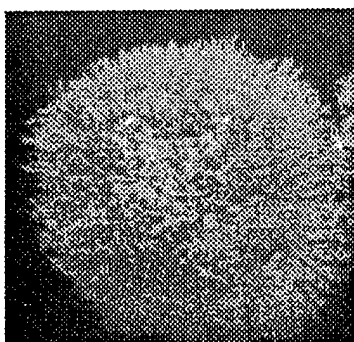
A)



B)



C)



D)

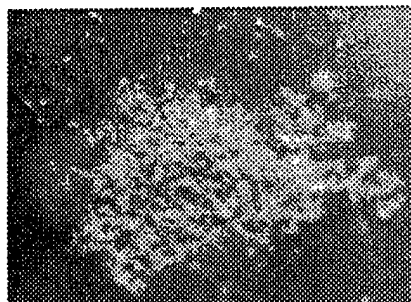


**Figure 6.** Photographs of Ti coupons subjected to electrodisolution with conical tip graphite cathode in 1M NaCl as a function of XC72R volume concentration. A) 0%, B) 15%, C) 25%, and D) 45% XC72R.

## **Task 2      *Fabrication of and Performance Improvement to Cell for Electrochemical Machining***

The objective of work performed in this task was to design and fabricate a prototype ECM lathe, a schematic of which is shown in Figure 7. This prototype ECM lathe contained several key components, including 1) an anode-cathode chamber, 2) a power supply, 3) a pressure vessel for delivering heterogeneous electrolyte via a hole in the cathode (tool) to the titanium alloy anode being machined, and 4) a means of translating the cathode relative to the anode.

Specifically the ECM lathe incorporated a 20A, 55V power supply (Kepco), interfaced to a computer for collection of current and voltage data. The anode consisted of the titanium alloy of interest which was mounted on a polycarbonate holder. The cathode was either a W(72%)/Cu(28%) tube with 3.15mm o.d. and 0.85mm i.d. or a copper tube with 3.2mm o.d. and 1.65mm i.d. The electrolyte/particle slurry was delivered from a stainless steel vessel of volume of 4 liters pressurized with compressed air and mediated through stainless steel tubing connected to the cathode through Teflon tubing to give the assembly flexibility during translation. The ECM region apparatus was enclosed in a polycarbonate shield and contained a Viton A seal supported on a polycarbonate disk. The splash shield assembly was supported

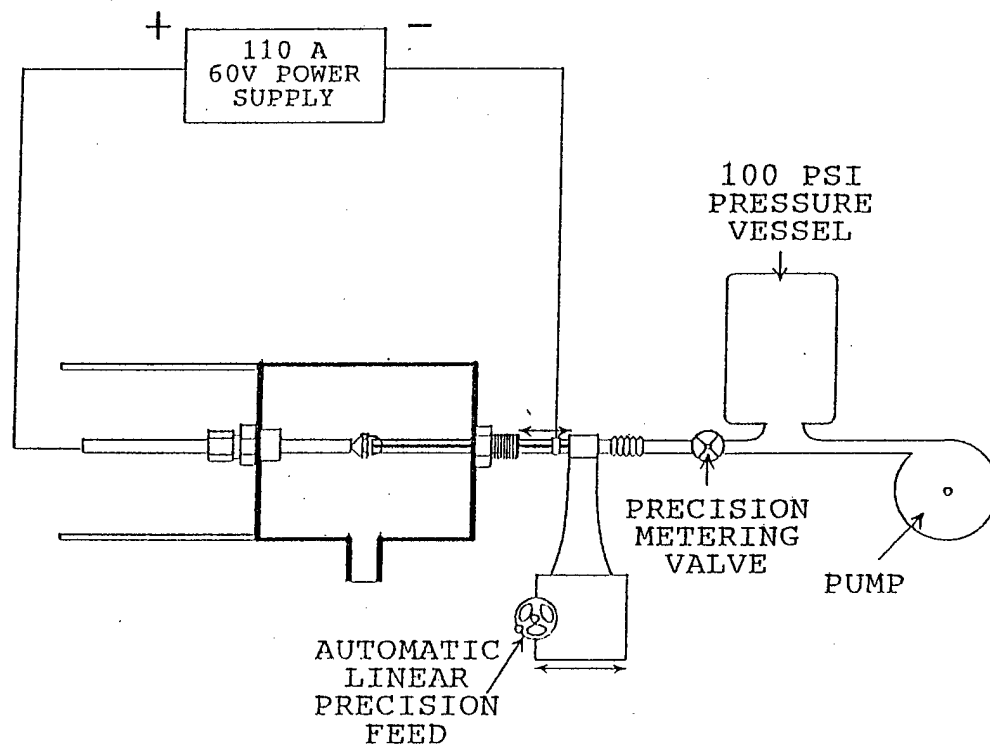


**Figure 7.**      Schematic of bench scale apparatus designed and fabricated during Phase I for electrochemically drilling holes into titanium and titanium alloys.

by a number of threaded tie rods. The cathode assembly was supported on a stepper motor (Superior Electric Slo-Syn indexer and stepper motor SP 155-A-6209) driven translational stage. Photographs of this prototype lathe are shown respectively in Figures 8 and 9.

#### **a) Preliminary ECM Results in the Absence of Heterogeneous Dispersants Within the Aqueous Electrolyte**

Preliminary experimental measurements performed using this ECM lathe in the absence of dispersed particles within the ionically conducting aqueous electrolyte (flow rate 7ml/sec) are summarized in Table 2. Coupons of Ti, Ti 6-4, and Ti 6242 were subjected to hole boring in electrolytes possessing the respective compositions 1M NaCl and 1.05M NaBr/0.42M NaNO<sub>3</sub>. Conditions of stationary and moving cathode were employed in separate experiments and the dependence of ECM on drilling speed examined. For titanium metal removal in 1M NaCl, where the initial interelectrode spacing was 400 microns, translation of the cathode (0.0017mm/sec) towards the anode was not found to enhance material removal rate when the cathode was stationary. This was a consequence of the relatively large interelectrode spacing initially selected. Shape resolution was less defined when using a translating cathode again because of this large interelectrode spacing. Using 1.05M NaBr/0.42M NaNO<sub>3</sub>, material removed from a titanium coupon increased from  $1.343 \times 10^{-4}$ g/C with a stationary bit to  $1.390 \times 10^{-4}$ g/C at 0.0015mm/sec, followed by a decrease to  $1.377 \times 10^{-4}$ g/C at 0.002mm/sec. (Coupons 17-20 in Table 2).

In the case of the ECM Ti 6-4 in 1M NaCl, a cathode tool speed of 0.0026mm/sec produced greater material removal ( $1.269 \times 10^{-4}$  g/C) rates than did a stationary bit ( $1.13 \times 10^{-4}$  g/C). The loss of shape resolution (i.e. increased cut diameter and reduced cut depth) was not severe. In 1.05M NaBr/0.42 M NaNO<sub>3</sub>, material removal was again higher ( $1.382 \times 10^{-4}$ g/C vs.  $1.353 \times 10^{-4}$  g/C) with moving (0.0026mm/sec) as opposed to a stationary cathode. The ECM of Ti 6242 in 1.05M NaBr/0.42M NaNO<sub>3</sub> did not appear to be significantly influenced by cathode translational speed.

Data for the alloy 76%Ti-15%V-3%Sn-3%Cr-3%Al (coupons 2-13) using anode-cathode spacings varying from 48 to 1000 microns showed that smaller cut diameters (better shape resolution) were obtained with translating (of 0.0027mm/sec) as opposed to a stationary cathode. Cut diameters were uniformly smaller for the translating cathode than for a stationary cathode. In the case of this alloy, this improvement is apparently due to the overall lower and constant resistance obtained with the translating cathode.

In the absence of heterogeneous particles within the aqueous electrolyte, preliminary experiments using this one axis ECM lathe showed that some dependence of material removal on drilling speed was obtained, but that shape resolution was lost as the bit was advanced into the cut (in the case of NaBr/NaNO<sub>3</sub>). Material removal was not significantly different between NaCl and NaBr/NaNO<sub>3</sub> electrolytes. However, NaCl demonstrated a favorable effect on maintaining or improving shape resolution when a translating cathode was utilized.

#### **b) Implementation of Experimental Design for ECM in Heterogeneous Electrolytes**

The influence of experimental variables on the ECM of titanium alloys was assessed

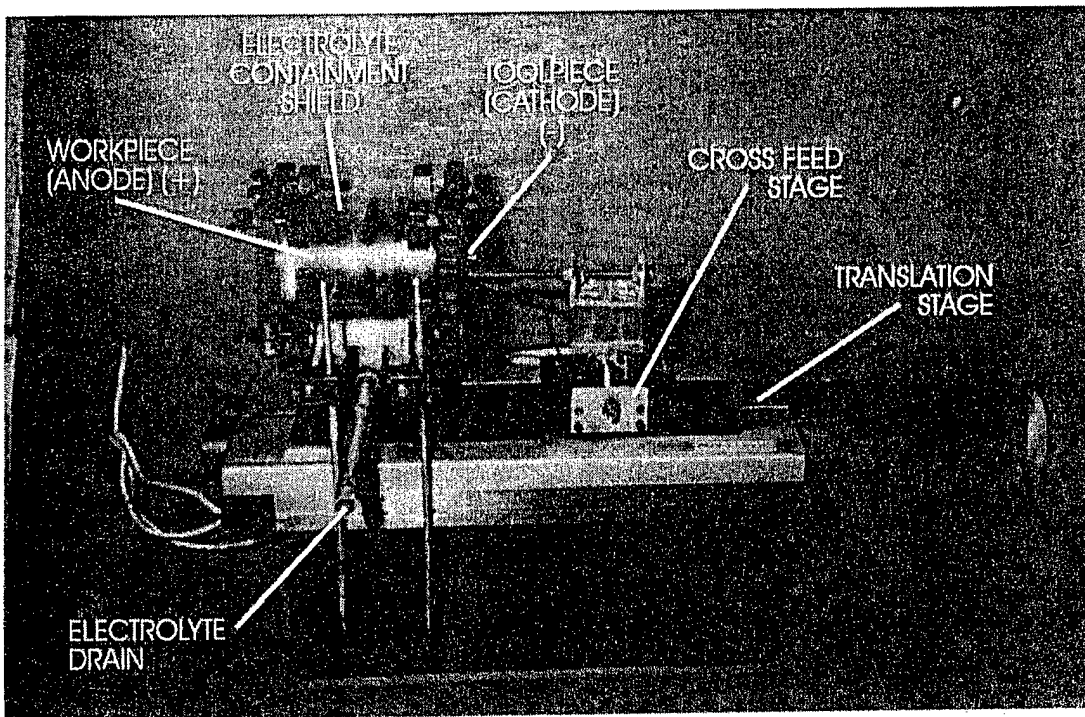


Figure 8. Photograph of prototype ECM lathe fabricated at Eltron incorporating a stepper motor driven translational stage.

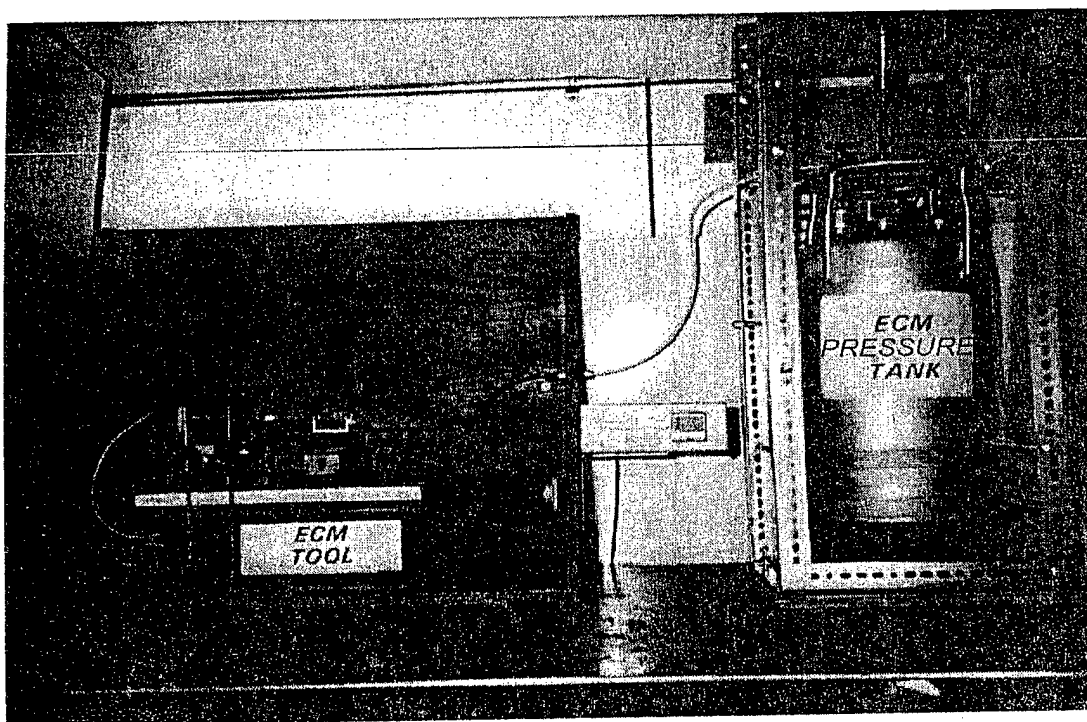


Figure 9. Photograph of overall ECM lathe assembly used during performance of Phase I for the machining of titanium alloys.

**Table 2.**  
**Preliminary Experimental Results Obtained on Selected Titanium Alloys Using a**  
**One-Axis ECM Lathe In the Absence of Electronically Conducting Particulates**

Coupon #	Material	Apparatus	Btu Type	Electrolyte Used	Coupon Weight Loss (grams)	Current Applied (mAmps)	Length of Trial (Sec)	Charge Applied (Coulombs)	Volume Electrolyte (ml)	Material Removed per charge (grams/coulomb)	Cut Depth (mm)	Cut Diameter (mm)	Bit to Coupon	
													Distance (microns)	Bit Speed (mm/sec)
1	Titanium (99.6 + % Pure)	ECM Tool	Copper Tube	1M NaCl	0.0841	1000	600	600	4150	0.0001402	1.016	6.553	400	N/A
2	76% Ti-15% V-3% Sn-3% Cr-3% Al	ECM Tool	Copper Tube	1M NaCl	0.0816	1000	600	600	4100	0.000136	1.676	5.41	400	N/A
3	76% Ti-15% V-3% Sn-3% Cr-3% Al	ECM Tool	Copper Tube	1M NaCl	0.0825	1000	600	600	4050	0.0001375	1.626	5.486	48	N/A
4	76% Ti-15% V-3% Sn-3% Cr-3% Al	ECM Tool	Copper Tube	1M NaCl	0.081	1000	600	600	4050	0.000135	1.651	6.147	100	N/A
5	76% Ti-15% V-3% Sn-3% Cr-3% Al	ECM Tool	Copper Tube	1M NaCl	0.0799	1000	600	600	4060	0.0001332	1.651	6.312	200	N/A
6	76% Ti-15% V-3% Sn-3% Cr-3% Al	ECM Tool	Copper Tube	1M NaCl	0.0658	500 to 1000	600	492	4100	0.0001337	1.321	5.804	800	N/A
7	76% Ti-15% V-3% Sn-3% Cr-3% Al	ECM Tool	Copper Tube	1M NaCl	0.0357	500	600	300	4125	0.000119	0.813	7.099	1000	N/A
8	76% Ti-15% V-3% Sn-3% Cr-3% Al	ECM Tool	Copper Tube	1M NaCl	0.0837	1000	600	600	3950	0.0001395	1.524	5.245	48	0.0027
9	76% Ti-15% V-3% Sn-3% Cr-3% Al	ECM Tool	Copper Tube	1M NaCl	0.0795	1000	600	600	3950	0.0001325	1.499	4.864	100	0.0028
10	76% Ti-15% V-3% Sn-3% Cr-3% Al	ECM Tool	Copper Tube	1M NaCl	0.0789	1000	600	600	4000	0.0001315	1.346	5.042	200	0.0028
11	76% Ti-15% V-3% Sn-3% Cr-3% Al	ECM Tool	Copper Tube	1M NaCl	0.0821	1000	600	600	4000	0.0001368	1.422	5.182	400	0.0027
12	76% Ti-15% V-3% Sn-3% Cr-3% Al	ECM Tool	Copper Tube	1M NaCl	0.0775	1000	600	600	3975	0.0001292	1.27	6.248	800	0.0027
13	76% Ti-15% V-3% Sn-3% Cr-3% Al	ECM Tool	Copper Tube	1M NaCl	0.0803	1000	600	600	4075	0.0001338	1.295	6.375	1000	0.0027
14	Titanium (99.6 + % Pure)	ECM Tool	Copper Tube	1M NaCl	0.0781	1000	600	600	4010	0.0001302	1.219	6.68	400	0.0017
15	90% Ti-6% Al-4% V	ECM Tool	Copper Tube	1M NaCl	0.0678	1000	600	600	4110	0.000113	1.575	4.826	400	N/A

**Table 2, Continued . . . . .**  
**Preliminary Experimental Results Obtained on Selected Titanium Alloys Using a**  
**One Axis ECM Lathe In the Absence of Electronically Conducting Particulates**

Coupon #	Material	Apparatus	Bit Type	Electrolyte Used	Coupon Weight Loss (grams)	Current Applied (mAmps)	Length of Trial (Sec)	Charge Applied (Coulombs)	Volume Electrolyte (mL)	Material Removed per charge (grams/coulomb)	Cut Depth (mm)	Cut Diameter (mm)	Bit to Coupon	
													Distance (microns)	Bit Speed (mm/sec)
16	90% Ti-6% Al-4% V	ECM Tool	Copper Tube	1M NaCl	0.0754	600 to 1000	600	594	4040	0.0001269	1.422	5.08	400	0.0026
17	Titanium (99.6+ % Pure)	ECM Tool	Copper Tube	1.05M NaBr-0.42M NaNO <sub>3</sub>	0.0806	1000	600	600	3950	0.0001343	1.778	5.753	400	N/A
18	Titanium (99.6+ % Pure)	ECM Tool	Copper Tube	1.05M NaBr-0.42M NaNO <sub>3</sub>	0.0811	1000	600	600	3875	0.0001352	1.27	6.274	400	0.0027
19	Titanium (99.6+ % Pure)	ECM Tool	Copper Tube	1.05M NaBr-0.42M NaNO <sub>3</sub>	0.0826	1000	600	600	3900	0.0001377	1.27	5.88	400	0.002
20	Titanium (99.6+ % Pure)	ECM Tool	Copper Tube	1.05M NaBr-0.42M NaNO <sub>3</sub>	0.0834	1000	600	600	3935	0.000139	1.219	6.553	400	0.0015
21	76% Ti-15% V-3% Sn-3% Cr-3% Al	ECM Tool	Copper Tube	1.05M NaBr-0.42M NaNO <sub>3</sub>	0.0824	720 to 1000	600	588.8	4025	0.0001399	1.981	5.029	400	N/A
22	76% Ti-15% V-3% Sn-3% Cr-3% Al	ECM Tool	Copper Tube	1.05M NaBr-0.42M NaNO <sub>3</sub>	0.0899	1000	600	600	4010	0.0001498	1.422	6.02	400	0.0025
23	90% Ti-6% Al-4% V	ECM Tool	Copper Tube	1.05M NaBr-0.42M NaNO <sub>3</sub>	0.0812	1000	600	600	4000	0.0001353	1.88	5.436	400	N/A
24	90% Ti-6% Al-4% V	ECM Tool	Copper Tube	1.05M NaBr-0.42M NaNO <sub>3</sub>	0.0829	1000	600	600	4015	0.0001382	1.422	5.537	400	0.0016
25	86% Ti-6% Al-2% Mo-4% Zr-2% Sn	ECM Tool	Copper Tube	1.05M NaBr-0.42M NaNO <sub>3</sub>	0.089	1000	600	600	4005	0.0001483	1.829	5.461	400	N/A
26	86% Ti-6% Al-2% Mo-4% Zr-2% Sn	ECM Tool	Copper Tube	1.05M NaBr-0.42M NaNO <sub>3</sub>	0.0905	1000	600	600	4000	0.0001508	1.321	5.588	400	0.015

as a function of heterogeneous electrolyte composition. An experimental design consisted of a matrix of experiments of which various combinations of variables were performed to determine the influence of these variables on the experimental outcome. Instead of using a factorial design as originally planned, which would have required  $2^{2N-1}$  (where  $N$  = number of experimental variables) experiments for a half-factorial design, a Plackett-Burman<sup>19</sup> design was utilized. In this statistical design,  $N-1$  experimental variables permitted us to determine their relative influence upon experimental results in only  $N$  experiments. During the course of this Phase I program, eleven experimental variables were identified as shown in Table 3, which were anticipated to account for almost all of the experimental variance. For the Plackett-Burman approach, only 12 experiments (conducted in replicate) were required to determine the relative influence of experimental variables upon ECM performance of titanium alloys, absent of any interaction terms. The resulting linear model could be represented in the form:

$$Y = b_1X_1 + b_2X_2 + b_3X_3 + \dots + b_iX_i \quad (1)$$

where  $b_i$  were coefficients of the corresponding experimental variables  $X_i$ . The design matrix employed in this program is presented in Table 3.

Eleven variables examined in the program corresponded to temperature ( $X_1$ ), initial interelectrode spacing ( $X_2$ ), electrolyte velocity ( $X_3$ ), current density ( $X_4$ ), particle concentration ( $X_5$ ), electrolyte type ( $X_6$ ), electrolyte concentration ( $X_7$ ), particle type ( $X_8$ ), cathode translational speed ( $X_9$ ), titanium designation ( $X_{10}$ ), and particle size ( $X_{11}$ ). Independent variables such as electrolyte, particle, and alloy type and dependent variables such as the presence or absence of pitting (i.e., those presenting a dilemma) were represented by a dummy variable. By a dummy variable we mean, a number assigned arbitrarily to a variable which cannot readily be assigned a numerical value. High (+) and low (-) values were variables experimentally determined such that they were in accord with experimental reasonableness. Results obtained from these designed experiments are presented in Table 4.

With this approach mere observation of data could not provide information sufficient to draw conclusions about the contribution of each variable to variance in ECM performance on selected titanium alloys. Consequently, ANalysis Of VAriance (ANOVA)<sup>19</sup> or multiple regression analysis was performed. The latter approach (multiple regression) was employed, using equation 1 as the model. However, prior to this analysis, data was transformed into z-scores, ( $z$ ) which was defined by dividing the deviation for a variable from its mean value by the standard derivation ( $\sigma_i$ ) of that variable as shown in equation 2:

$$z_i = \frac{x_i - x_{mean}}{\sigma_i} \quad (2)$$

This z-transformed data (replicate runs averaged) is summarized in Table 5 and was fit to the model given by equation 1. Resulting unadjusted and adjusted multiple regression correlation coefficients are presented in Table 6.

These coefficients showed that experimental results for ECM were correlated with experimental variables in the following order of decreasing strength: mean cell voltage > cut



Table 3.  
Plackett-Burman Experimental Design for ECM of Titanium Alloys

Plackett Burman Design											
Variable #											
Expt#	X <sub>1</sub>	X <sub>2</sub>	X <sub>3</sub>	X <sub>4</sub>	X <sub>5</sub>	X <sub>6</sub>	X <sub>7</sub>	X <sub>8</sub>	X <sub>9</sub>	X <sub>10</sub>	X <sub>11</sub>
1	+	+	-	+	+	+	-	-	-	+	-
2	-	+	+	-	+	+	+	-	-	-	+
3	+	-	+	+	-	+	+	+	-	-	-
4	-	+	-	+	+	-	+	+	+	-	-
5	-	-	+	-	+	+	-	+	+	+	-
6	-	-	-	+	-	+	+	-	+	+	+
7	+	-	-	-	+	-	+	+	-	+	+
8	+	+	-	-	-	+	-	+	+	-	+
9	+	+	+	-	-	-	+	-	+	+	-
10	-	+	+	+	-	-	-	+	-	+	+
11	+	-	+	+	+	-	-	-	+	-	+
12	-	-	-	-	-	-	-	-	-	-	-
X <sub>1</sub>	Temperature	+ 100°C		- 25°C							
X <sub>2</sub>	Initial gap spacing	500 microns		50 microns							
X <sub>3</sub>	Electr. Velocity	400cm/s		100cm/s							
X <sub>4</sub>	Current Density	35A/cm <sup>2</sup>		3.5mA/cm <sup>2</sup>							
X <sub>5</sub>	Particle Concentration	0		25V%							
X <sub>6</sub>	Electr. type	NaNO <sub>3</sub> /NaBr		NaBr							
X <sub>7</sub>	Electr. conc.	4.4		0.5M							
X <sub>8</sub>	Particle type	MnO <sub>2</sub>		XC72R							
X <sub>9</sub>	Cathode speed	0.003mm/sec		0							
X <sub>10</sub>	Metal	Ti 6242		Ti							
X <sub>11</sub>	Particle size	100 microns		70 angstroms							

**Table 4.**  
**Results Obtained from Experiments Conducted According to Plackett-Burman Design**  
**To Determine Influence of Heterogeneous Electrolyte on ECM**

Coupon #	Material	Electrolyte Used	Coupon Wt Loss (g)	Tank Pressure (psig)	Current Applied (mA)	Charge Applied (g)	Volume Electrolyte (ml)	Material Removed per Charge (grams/coulomb)	Linear Velocity (cm/sec)	Force on Coupon (Newtons/cm <sup>2</sup> )	Drilling Speed (mm/sec)	Cut Depth (mm)	Cut Diameter (mm)	Bit / Coupon		Temp (°C)
														Distance	Speed	
44	Titanium (99.6+ % Pure)	0.5 M NaBr	0.0392	3	1000	300	700	1.307e-04	109	0.1188	1.270e-04	0.038	5.258	48	N/A	26
45	Titanium (99.6+ % Pure)	0.5 M NaBr	0.0052	3	100	30	725	1.733e-04	113	0.1274	1.270e-04	0.038	4.496	48	N/A	25
46	Titanium (99.6+ % Pure)	0.5 M NaBr	0.0051	3	100	30	600	1.700e-04	93	0.0873	8.467e-05	0.025	4.039	48	N/A	23
47	8-6% Ti-6% Al-2% Mo4 % Zr-2% Sn	0.5 M NaBr	0.0415	33	1000	300	2075	1.383e-04	323	1.0436	2.455e-03	0.737	5.258	250	N/A	23
48	86% Ti-6% Al-2% Mo4 % Zr-2% Sn	0.5 M NaBr	0.0398	33	1000	300	2050	1.327e-04	319	1.0186	2.625e-03	0.787	5.334	250	N/A	23
49	86% Ti-6% Al-2% Mo4 % Zr-2% Sn	3.15M NaBr/1.26 M NaNO3	0.0441	3	1000	300	600	1.470e-04	93	0.0873	2.032e-03	0.610	5.334	48	0.002	23
50	86% Ti-6% Al-2% Mo4 % Zr-2% Sn	3.15M NaBr/1.26 M NaNO3	0.0444	3	1000	300	715	1.480e-04	111	0.1239	1.863e-03	0.559	5.563	48	0.002	23
51	Titanium (99.6+ % Pure)	3 M NaBr	0.0428	3	1000	300	750	1.427e-04	117	0.1363	1.947e-03	0.584	4.953	250	0.002	80
52	Titanium (99.6+ % Pure)	3 M NaBr	0.0412	3	1000	300	675	1.373e-04	105	0.1104	1.736e-03	0.521	5.156	250	0.002	80
53	86% Ti-6% Al-2% Mo4 % Zr-2% Sn	0.525 M NaBr/0.21 M NaNO3	0.0399	33	1000	300	Error	1.330e-04	0	0.0000	2.328e-03	0.699	5.004	48	0.002	80
54	86% Ti-6% Al-2% Mo4 % Zr-2% Sn	0.525 M NaBr/0.21 M NaNO3	0.0058	33	100	30	2650	1.933e-04	413	1.7021	1.270e-04	0.038	3.988	48	0.002	80
55	86% Ti-6% Al-2% Mo4 % Zr-2% Sn	0.525 M NaBr/0.21 M NaNO3	0.0063	33	100	30	2575	2.100e-04	401	1.6071	1.693e-04	0.051	3.620	48	0.002	80
56	Titanium (99.6% Pure)	3.15 M NaBr/1.26 M NaNO3	0.0024	33	100	30	1325	8.400e-05	206	0.4255	1.667e-04	0.050	2.860	250	0	80
61	Titanium (99.6% Pure)	3.15 M NaBr/1.26 M NaNO3	0.0050	33	100	30	1500	1.666e-04	234	0.5454	3.000e-04	0.090	2.970	250	0	80
62	Titanium (99.6% Pure)	3.15 M NaBr/1.26 M NaNO3	0.0057	33	100	30	1500	1.900e-04	234	0.5454	2.667e-04	0.080	2.880	250	0	80
69	86% Ti-6% Al-2% Mo4 % Zr-2% Sn	3 M NaBr w/5% vol MnO2	0.0045	3	100	30	Less 100	1.500e-04	15	0.0022	3.333e-05	0.010	5.000	50	0	80
70	86% Ti-6% Al-2% Mo4 % Zr-2% Sn	3 M NaBr w/5% vol MnO2	0.0128	33	100	30	Less 100	4.270e-04	15	0.0022	3.333e-05	0.010	4.210	50	0	80
71	86% Ti-6% Al-2% Mo4 % Zr2% Sn	3 M NaBr w/5% vol MnO2	0.0018	3	100	30	Less 100	6.000e-05	15	0.0022	3.333e-05	0.010	4.060	50	0	80

**Table 4, Continued . . . . .**  
**Results Obtained from Experiments Conducted According to Plackett-Burman Design**  
**To Determine Influence of Heterogeneous Electrolyte on ECM**

Coupon #	Material	Electrolyte Used	Coupon Wt Loss (g)	Tank Pressure (psig)	Current Applied (mA)	Charge Applied (C)	Volume Electrolyte (ml)	Material Removed per Charge (grams/coulomb)	Linear Velocity (cm/sec)	Force on Coupon (Newtons/cm <sup>2</sup> )	Drilling Speed (mm/sec)	Cut Depth (mm)	Cut Diameter (mm)	Bt (Coupon)		Temp (°C)
														Distance	Speed	
72	86% Ti-6% Al-2% Mo 4% Zr-2% Sn	3 M NaBr w/5% vol MnO <sub>2</sub>	0.0036	3	100	30	Less 100	1.200e-04	15	0.0022	3.333e-05	0.010	3.780	50	0	80
63	Titanium (99.6% Pure)	0.5MNaBr/NaNO <sub>3</sub> w/5% vol MnO <sub>2</sub>	0.0054	3	100	30	1000	1.800e-04	156	0.2424	3.333e-05	0.010	4.770	250	0.002	25
64	Titanium (99.6% Pure)	0.5MNaBr/NaNO <sub>3</sub> w/5% vol MnO <sub>2</sub>	0.0053	3	100	30	1000	1.770e-04	156	0.2424	1.667e-04	0.050	4.540	250	0.002	25
57	86% Ti-6% Al-2% Mo 4% Zr-2% Sn	3M NaBr w/25% vol XC72R	0.0055	33	100	30	1650	1.830e-04	257	0.6599	3.333e-05	0.010	4.330	250	0	25
58	86% Ti-6% Al-2% Mo 4% Zr-2% Sn	3M NaBr w/25% vol XC72R	0.0040	33	100	30	1300	1.330e-04	202	0.4096	3.333e-05	0.010	4.030	250	0.002	25
59	86% Ti-6% Al-2% Mo 4% Zr-2% Sn	3M NaBr w/25% vol XC72R	0.0040	33	100	30	1500	1.330e-04	234	0.5454	3.333e-05	0.010	4.720	250	0	25
60	86% Ti-6% Al-2% Mo 4% Zr-2% Sn	3M NaBr w/25% vol XC72R	0.0050	33	100	30	1250	1.660e-04	195	0.3787	3.333e-05	0.010	3.870	250	0.002	25
65	86% Ti-6% Al-2% Mo 4% Zr-2% Sn	0.5MNaBr/NaNO <sub>3</sub>	0.0472	3	1000	300	1000	1.570e-04	156	0.2424	2.667e-03	0.800	5.860	250	0	80
66	86% Ti-6% Al-2% Mo 4% Zr-2% Sn	0.5MNaBr/NaNO <sub>3</sub> w/25% vol XC72R	0.0468	3	1000	300	1000	1.560e-04	156	0.2424	2.000e-03	0.600	5.230	250	0	80
67	Titanium (99.6% Pure)	3.15 M NaBr/1.26 M NaNO <sub>3</sub> w/5% vol MnO <sub>2</sub>	0.0402	33	1000	300	1700	1.340e-04	265	0.7005	2.333e-03	0.700	4.960	50	0	25
68	Titanium (99.6% Pure)	3.15 M NaBr/1.26 M NaNO <sub>3</sub>	0.0398	33	1000	300	1700	1.330e-04	265	0.7005	2.100e-03	0.630	5.170	50	0	25

Table 5.  
z-Transformed Data from Experiments Performed According to Plackett-Burman Design

Particle Conc.	Bit/Coupon Gap	Electrolyte Velocity	Current Density	Temp	Electrolyte	Electr. Conc.	Particle Type	Bit Speed	Alloy Type	Material Removal	Cut Depth	Cut Diameter	Pitting Y/N	Mean Cell V.	Highest Cell V.
-0.619	-1.044	-0.87	-0.87	-0.87	-1.044	-1.044	-1.044	-0.87	-1.044	0.535	-0.862	-0.409	-1.261	-0.552	-0.642
-0.609	0.87	1.044	1.044	-0.87	-1.044	-1.044	0.87	-0.87	0.87	-1.058	1.362	0.877	0.721	2.141	2.79
-0.609	-1.044	-0.87	1.044	-0.87	0.87	0.87	-1.044	1.044	0.87	-0.529	0.82	1.068	0.721	-0.297	-0.529
-0.609	0.87	-0.87	1.044	1.044	-1.044	0.87	0.87	1.044	-1.044	-0.86	0.723	0.576	-1.261	-0.388	-0.367
-0.609	-1.044	1.044	-0.87	1.044	0.87	-1.044	0.87	1.044	0.87	1.857	-0.823	-0.989	0.721	-0.722	-0.418
-0.609	0.87	1.044	-0.87	1.044	0.87	0.87	-1.044	-0.87	-1.044	-0.557	-0.735	-2.115	0.721	-0.713	-0.564
-0.094	-1.044	-0.87	-0.87	1.044	-1.044	0.87	0.87	-0.87	0.87	1.31	-0.928	-0.415	0.721	-0.907	-0.703
-0.094	0.87	-0.87	-0.87	-0.87	0.87	-1.044	0.87	1.044	-1.044	0.836	-0.867	0.076	-1.261	-0.714	0.351
1.968	0.87	1.044	-0.87	-0.87	-1.044	0.87	-1.044	1.044	0.87	-0.254	-0.928	-0.446	0.721	-0.664	-0.31
1.968	0.87	-0.87	1.044	1.044	0.87	-1.044	-1.044	-0.87	0.87	-0.133	1.173	1.189	0.721	0.236	-0.029
-0.094	-1.044	1.044	1.044	-0.87	0.87	0.87	0.87	-0.87	-1.044	-1.146	1.066	0.589	-1.261	0.881	0.421

Table 6.  
Multiple Regression Correlation Coefficients for Fits to Plackett Burman Data

Measured Result	Unadjusted R	Adjusted R
Material Removal	0.979	0.765
Cut Depth	0.9988	0.9874
Cut Diameter	0.95	0.1552
Pitting	0.9944	0.942
Mean Cell Voltage	0.9988	0.9881
Highest Cell Voltage	0.9853	0.8411

depth > the incidence of pitting > highest cell voltage encountered > material removal rate > cut diameter. From this the weakest correlation with ECM experimental variables was found for cut dispersion and the strongest being the mean cell voltage. Resulting coefficients are presented in ascending order in Table 7 where variables possessing largest magnitudes exert most influence upon ECM performance. Particle size was not used in this multiple regression analysis.

Another approach used in this program for determining the relative influence of experimental variables upon the ECM of titanium alloys was based upon use of a normal probability plot of the regression coefficients shown in Table 7. This was obtained by arranging coefficients in ascending order and calculating the normal probability from the relationship:

$$P = \frac{\# \text{ of coefficient } - \frac{1}{2}}{\text{total } \# \text{ of coefficients}} \quad (3)$$

Corresponding normal probability plots for the subject titanium alloys are presented in Figure 10 for A) material removal, B) cut depth, C) cut diameter, D) pitting extent, and E) mean cell voltage. Consideration of these plots, along with the magnitudes of the regression coefficients, led to the following conclusions:

- Cut diameter and cell voltage were sensitive to the presence of conductive particles within the aqueous electrolyte. The highest cell voltage observed had a negative coefficient of appreciable magnitude relative to other coefficients (i.e. an increasing concentration of particles tended to reduce cell voltage for ECM). XC72R tended to reduce cell voltage far more than MnO<sub>2</sub>.
- Particle concentration had a very substantial effect on pitting: increasing the concentration of particles lowered the tendency to pit. Only workpiece composition had a larger effect on pitting tendency. MnO<sub>2</sub> tended to suppress pitting to a greater extent than XC72R.
- Material removal and cut shape (depth and diameter) were most influenced by current density (i.e., the current density coefficient in equation 1 was largest). Material removal per unit charge was actually greater for lower current density. Cut depth and diameter were both increased with increasing current density.
- Pitting was most sensitive to the alloy type (e.g. the presence of Al, Mo, Zr, and Sn in Ti-6242 caused an increased propensity to pit).
- Cell voltage was most sensitive to anode-cathode gap: larger gaps, as expected produced higher cell voltages.

In addition to regression coefficients, magnitudes for outlying points on normal probability plots suggested that only current density, in the case of cut shape, and alloy type

Table 7.  
Dimensionless Multiple Regression Coefficients for Fit of Experimental Results  
Obtained from Plackett-Burman Design to Experimental Variables

Reg. Coeff	Material Removal	Norm. Prob.	Reg. Coeff	Cut Depth	Norm. Prob.	Reg. Coeff	Cut Diameter	Norm. Prob.	Reg. Coeff	Pitting	Norm. Prob.	Reg. Coeff	Mean Cell V	Norm. Prob.	Reg. Coeff	Highest Cell V	Norm. Prob.
b4	-0.604	0.055	b9	-0.138	0.055	b7	-0.252	0.055	b1	-0.372	0.055	b5	-0.604	0.055	b5	-0.565	0.055
b2	-0.452	0.167	b5	-0.054	0.1667	b2	-0.214	0.167	b4	-0.263	0.167	b9	-0.407	0.167	b9	-0.424	0.167
b7	-0.399	0.278	b7	-0.045	0.278	b5	-0.183	0.278	b9	-0.263	0.278	b7	-0.193	0.278	b1	-0.321	0.278
b6	0.012	0.389	b1	-0.034	0.389	b6	-0.154	0.389	b8	-0.215	0.389	b1	-0.178	0.389	b7	-0.155	0.389
b10	0.108	0.5	b8	0.032	0.5	b10	-0.018	0.5	b5	0.082	0.5	b6	0.188	0.5	b6	0.069	0.5
b1	0.151	0.611	b6	0.061	0.611	b8	0.12	0.611	b6	0.263	0.611	b10	0.244	0.611	b4	0.195	0.611
b8	0.172	0.722	b10	0.081	0.722	b9	0.172	0.722	b7	0.263	0.722	b4	0.325	0.722	b8	0.448	0.722
b9	0.229	0.833	b2	0.09	0.833	b1	0.331	0.833	b2	0.397	0.833	b8	0.453	0.833	b10	0.457	0.833
b5	0.327	0.944	b4	0.944	0.944	b4	0.87	0.944	b10	1.087	0.944	b2	0.512	0.944	b2	0.644	0.944

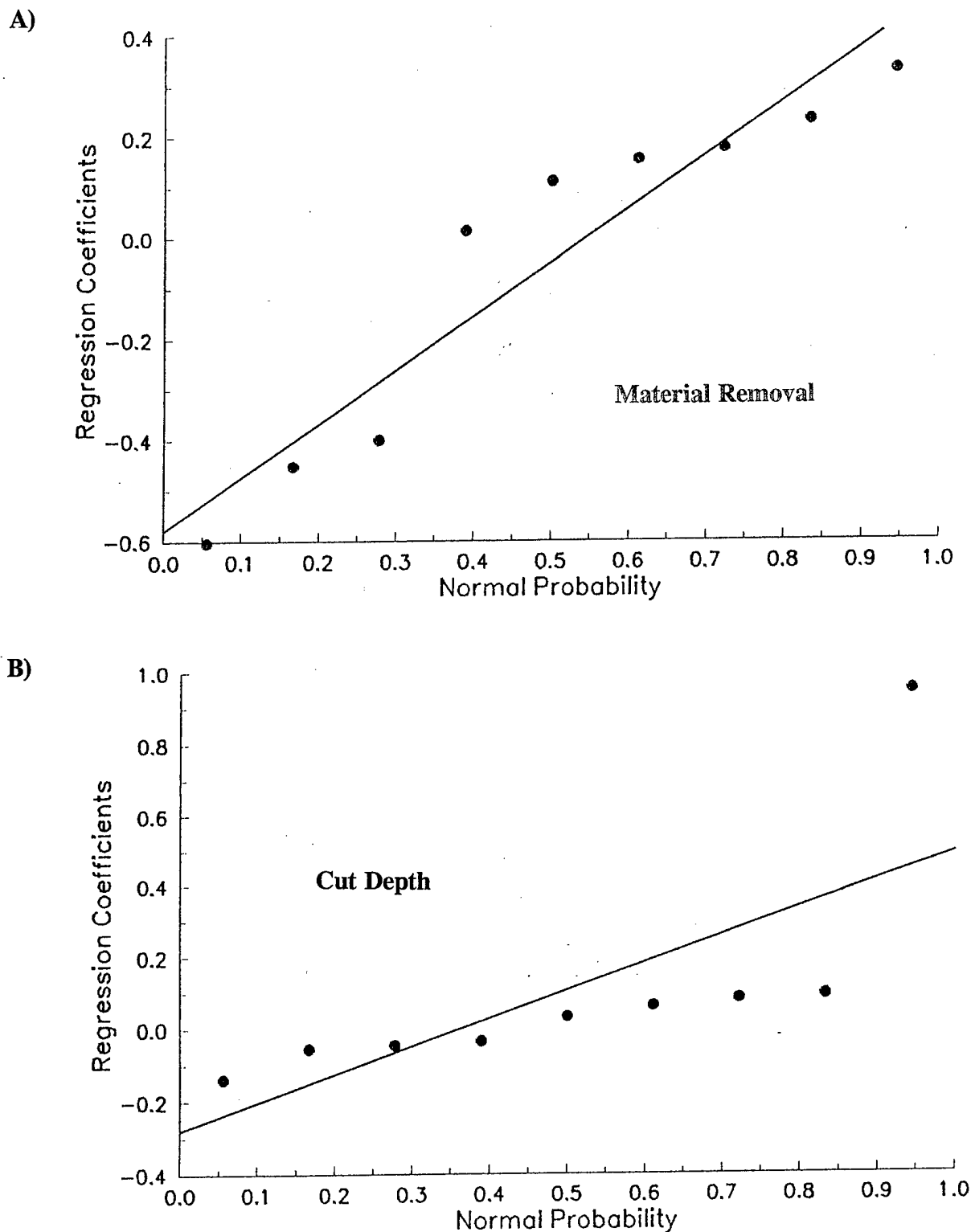


Figure 10. Normal probability plot for multiple regression coefficients obtained from Plackett-Burman experiments for A) material removal and B) cut depth.

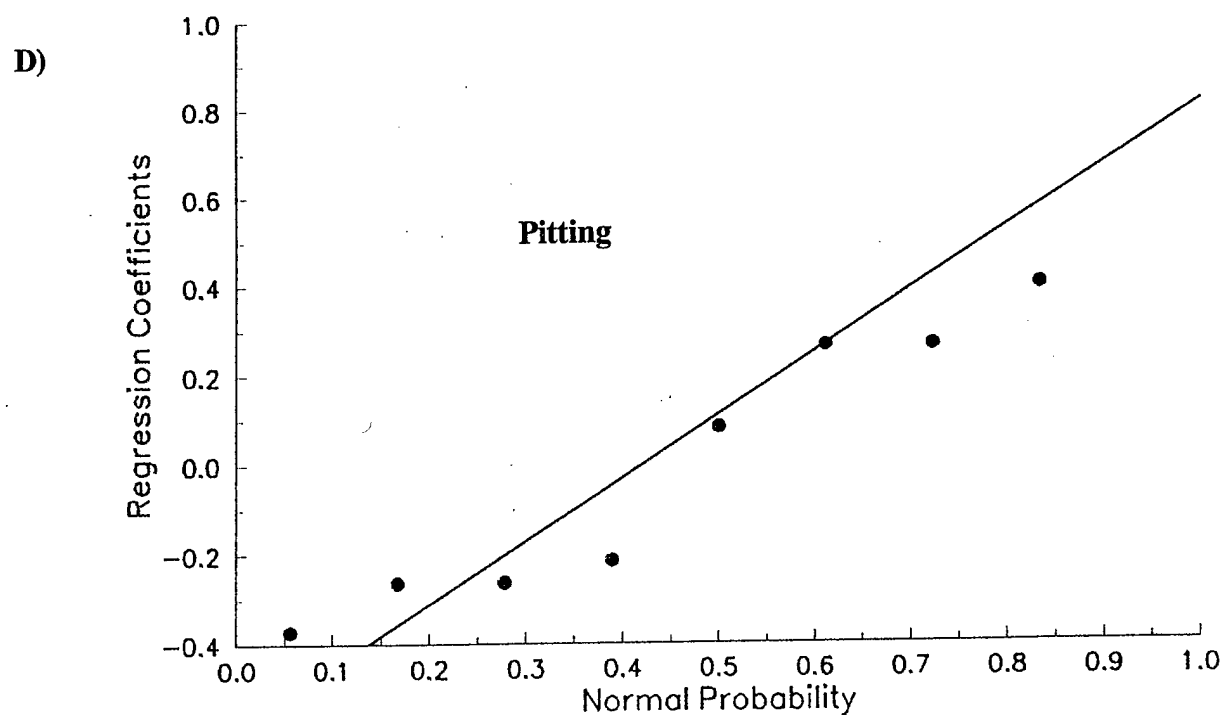
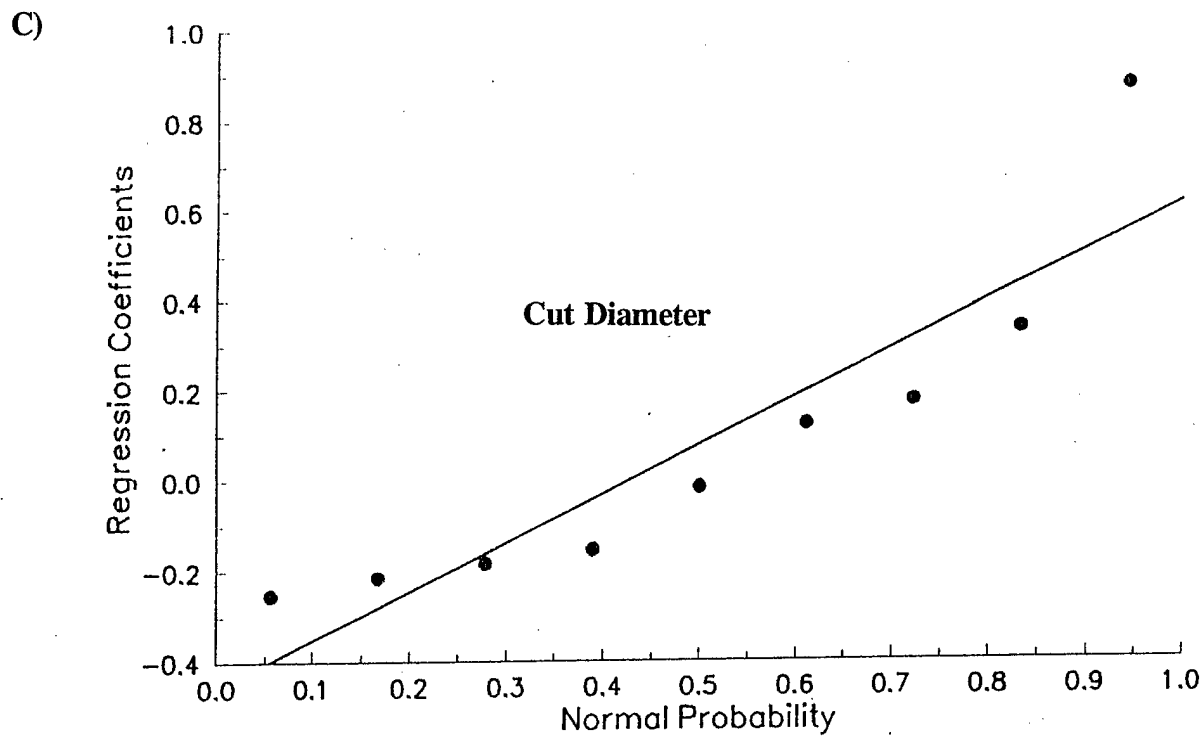


Figure 10, Cont'd. Normal probability plot for multiple regression coefficients obtained from Plackett-Burman experiments for C) cut diameter and D) pitting.



E)

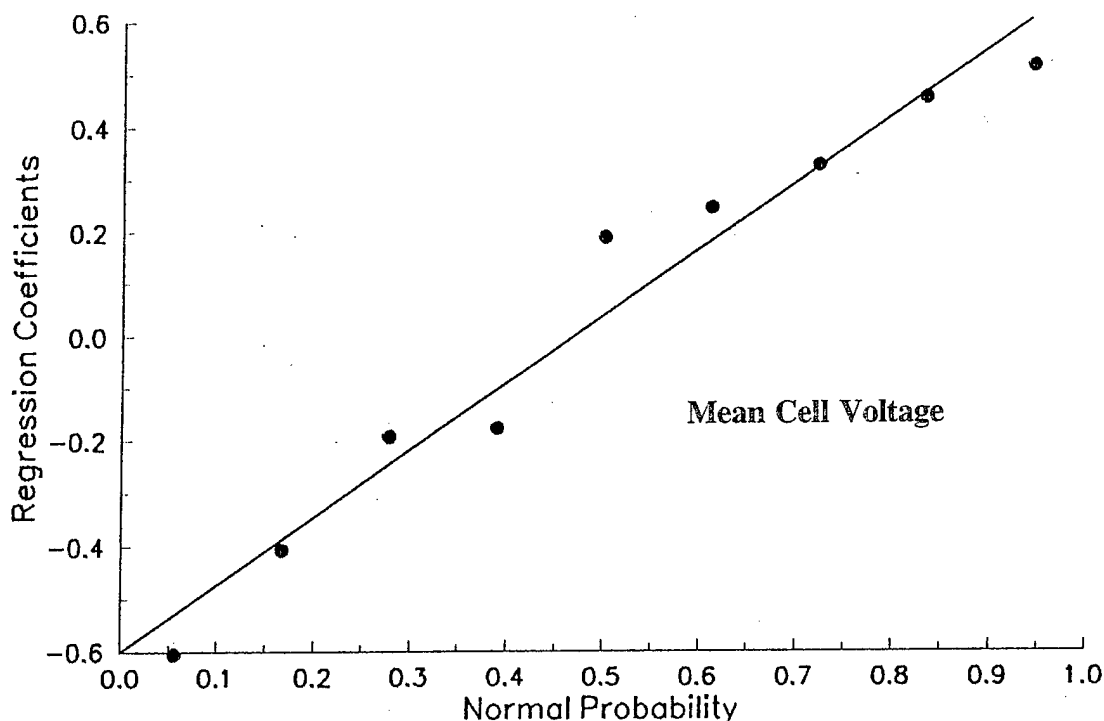


Figure 10, Cont'd. Normal probability plot for multiple regression coefficients obtained from Plackett-Burman experiments for E) mean cell voltage.

in the case of pitting, were substantially more influential than other factors. Consequently, in combination with the sensitivity analysis described above, results obtained were very helpful in determining subsequent experiments. Under conditions of defined anode-cathode gap these suggested experiments addressed during Phase I included 1) dependence of pitting, cell voltage, as well as other experimentally measurable quantities on concentration of particles XC72R (with or without heat treatment),  $\text{MnO}_2$ , Na zeolite-Y, and Ti metal dispersed within the aqueous electrolyte, 2) dependence of results on the type of alloy for each of the aforementioned particles, and 3) dependence of results on current density for each alloy-particle composition.

In overall conclusion to this experimental design, it may be said that 1) the Plackett-Burman design was found effective in determining the most influential variables among those sufficient to account for all experimental variance, 2) current density, alloy particle type and concentration were found variables exerting the most influence on ECM (as defined respectively by material removal, cut depth and particle diameter, occurrence of pitting, and cell voltage), and 3) alloy type, particle type, and particle concentration were selected as being variables to be subsequently examined during performance of this program.

To test the effect of adding alloying elements on the ECM properties of titanium alloys examined, the ECM of pure (99.6% Ti) was examined using the same particulate additives

as for Ti 6242 and Ti 6-4. Data for this material using untreated XC72R is given in Figure 11. In this case, the cell voltage decreased markedly between 15 and 35% XC72R followed by an increase above the particle-free voltage. The material removal increased with addition of untreated XC72R to a value as much as 25% greater than the particle-free case. The cut dispersion and degree of pitting was also markedly reduced. In fact, at 35vol% XC72R and above both diameter of the pit-affected area and the number of pits decreased substantially. At 65vol% XC72R, the cut was strongly focused about the tip of the conical cathode. All of these effects appeared to be greater for Ti than for Ti 6-4 or Ti 6242. These effects are shown photographically in Figure 12. The addition of carbon resulted in increased roughness (poorer surface finish), as demonstrated by Scanning Electron Micrographs. Roughness features of the order of  $10\mu\text{m}$  within the center of the cut were obtained with 65vol% XC72R, considerably greater than the  $\sim 1\mu\text{m}$  surface features obtained in the absence of carbon. However, in the latter case (absent XC72R), preferential grain boundary exposure (intergranular attack) was evident.

Similar effects, as obtained with untreated XC72R, were obtained with XC72R after heat treated at  $500^\circ\text{C}$ . This data is presented in Figure 13. Again, this data shows significant reductions in cut dispersion, extent of pitting, and required ECM cell voltage. However, less enhancement of material removal was obtained.

Photographs of coupons subjected to these experiments are presented in Figure 14. In contrast to cuts obtained with untreated XC72R, those using heat treated XC72R produced even less pitting, as is evident from the photographs. This is apparently associated with the lower oxygen scavenging capability of the heat treated carbon.

The use of oxidic additives was found to impart far less in the way of favorable characteristics to ECM than did carbon in its initial or surface oxidized forms. Data for the ECM of Ti in aqueous electrolyte containing Na zeolite-Y and  $\text{MnO}_2$  are presented in Figures 15 and 16, respectively.

In either case, cell voltage was increased, but more extensively with  $\text{MnO}_2$ . However, material removal was significantly enhanced in both cases. Cut diameter demonstrated an overall decrease with particle concentration. However, in marked contrast to the use of XC72R carbon the extent of pitting was markedly enhanced.

Ti 6-4(90%Ti/6%Al/4%V) was examined using the same protocol as employed for Ti 6242. Data for the ECM of Ti 6-4 in the presence of Na zeolite-Y is presented in Figure 17. In contrast to Ti 6242, Ti 6-4 exhibited much less dependence of cell voltage upon zeolite concentration within the aqueous electrolyte. Conversely, cut focusing was more pronounced in Ti 6-4. The degree of pitting was actually substantially reduced over that obtained with Ti 6242. Unlike Ti 6242, Ti 6-4 displayed overall material removal enhancement as a function of increased Na zeolite-Y concentrations.

Data for the ECM of Ti 6-4 in aqueous electrolyte incorporating heat treated XC72R is presented in Figure 18. This resulted in substantial reduction in cell voltage without a commensurate reduction in material removal, which was rather uniform with added XC72R concentration. Cut dispersion reached a minimum at 45vol% XC72R. Above 25% XC72R, the extent of pitting was markedly diminished. These results tend to suggest that the presence of Zr or Mo (as in Ti 6242) caused the formation of an insulating, passive film.

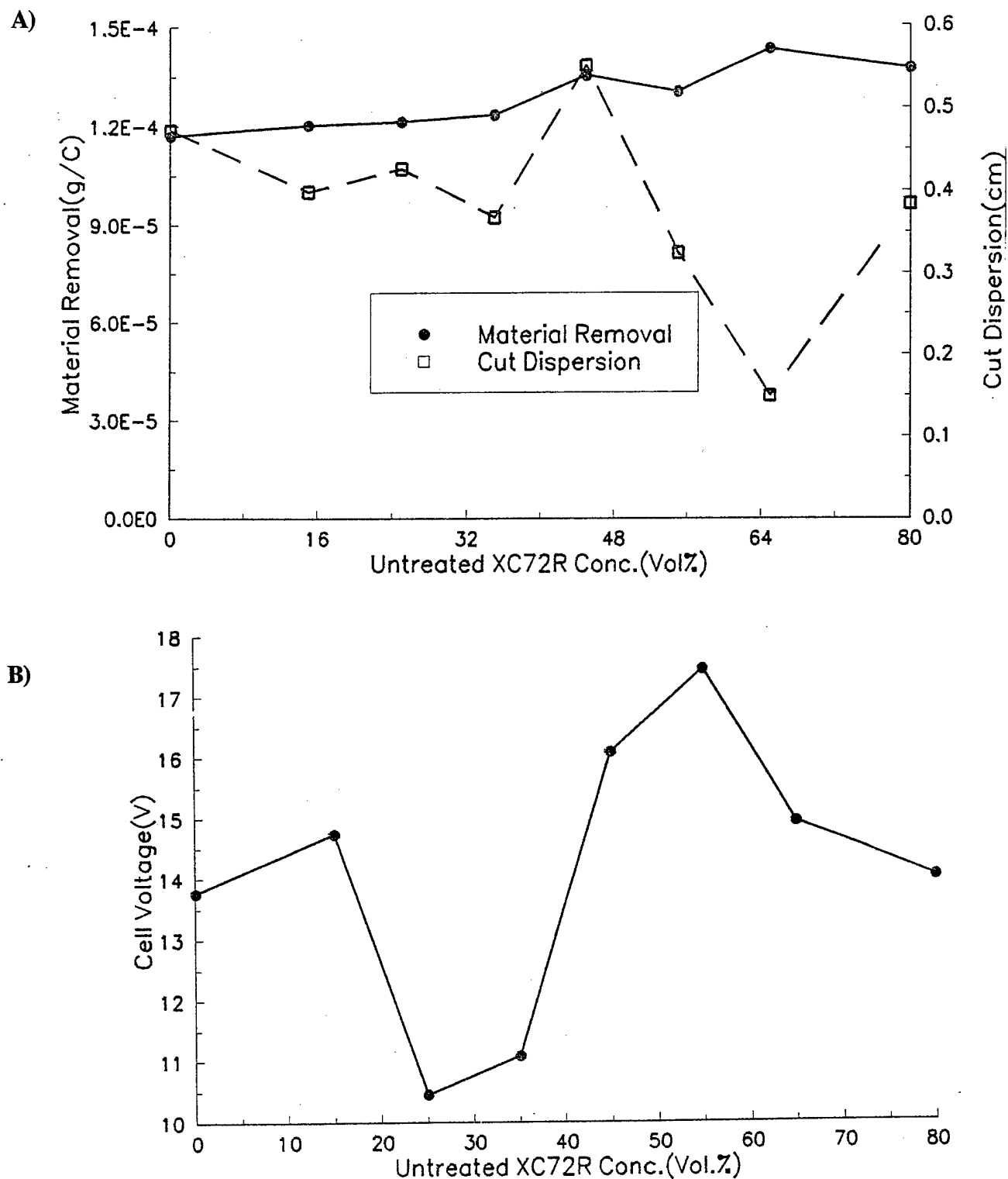


**Figure 11.** Material removal, cut dispersion, and cell voltage data for the ECM of Ti using untreated XC72R particles. Aqueous electrolyte: 3.15M NaBr/1.26M NaNO<sub>3</sub>.

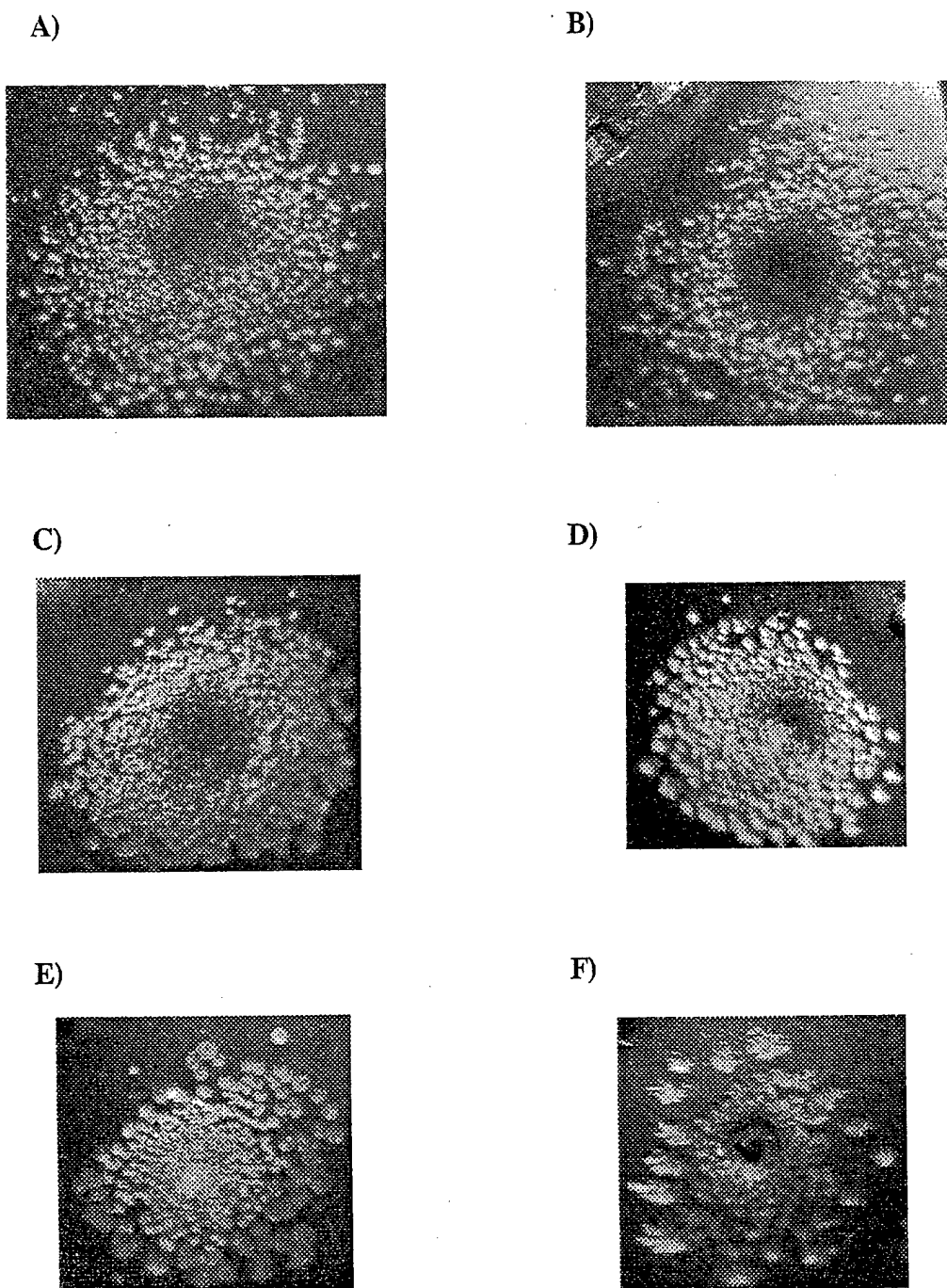


Figure 12. Photographs of Ti coupons subjected to electrodisso- lution in 3.15M NaBr/1.26M NaNO<sub>3</sub> with A) 0%, B) 15%, C) 25%, D) 35%, E) 55%, and F) 65% untreated XC72R (by volume). Uniform magnification was used for all photographs.

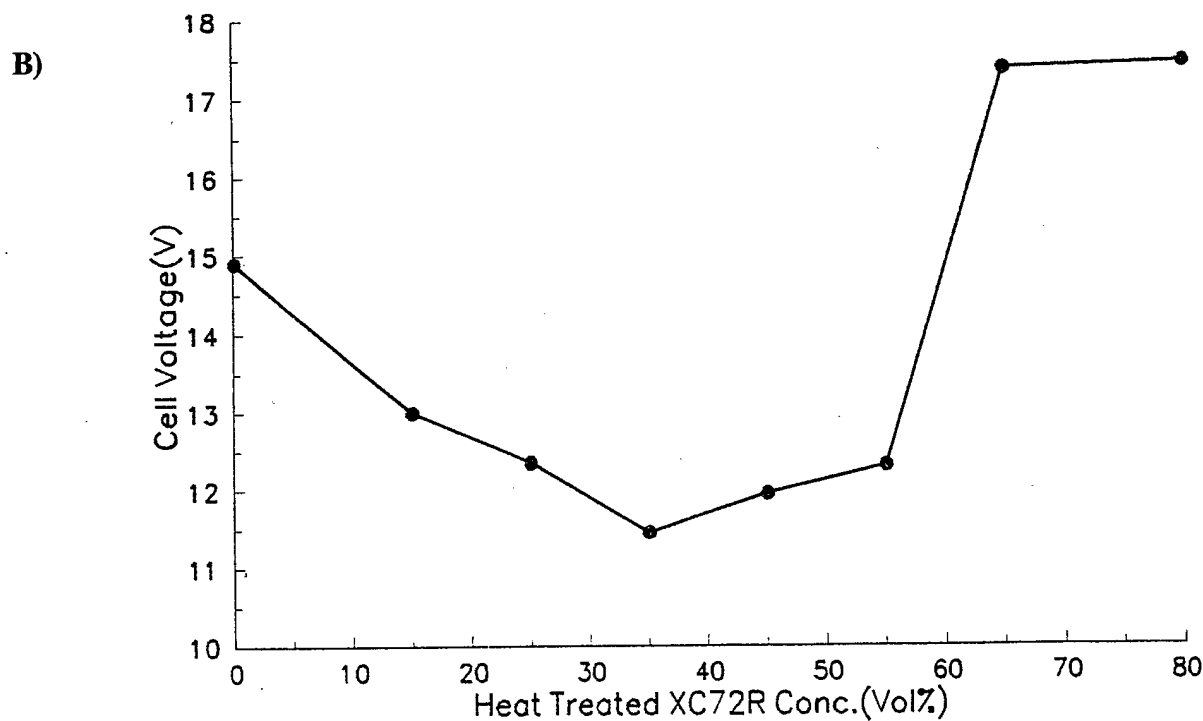
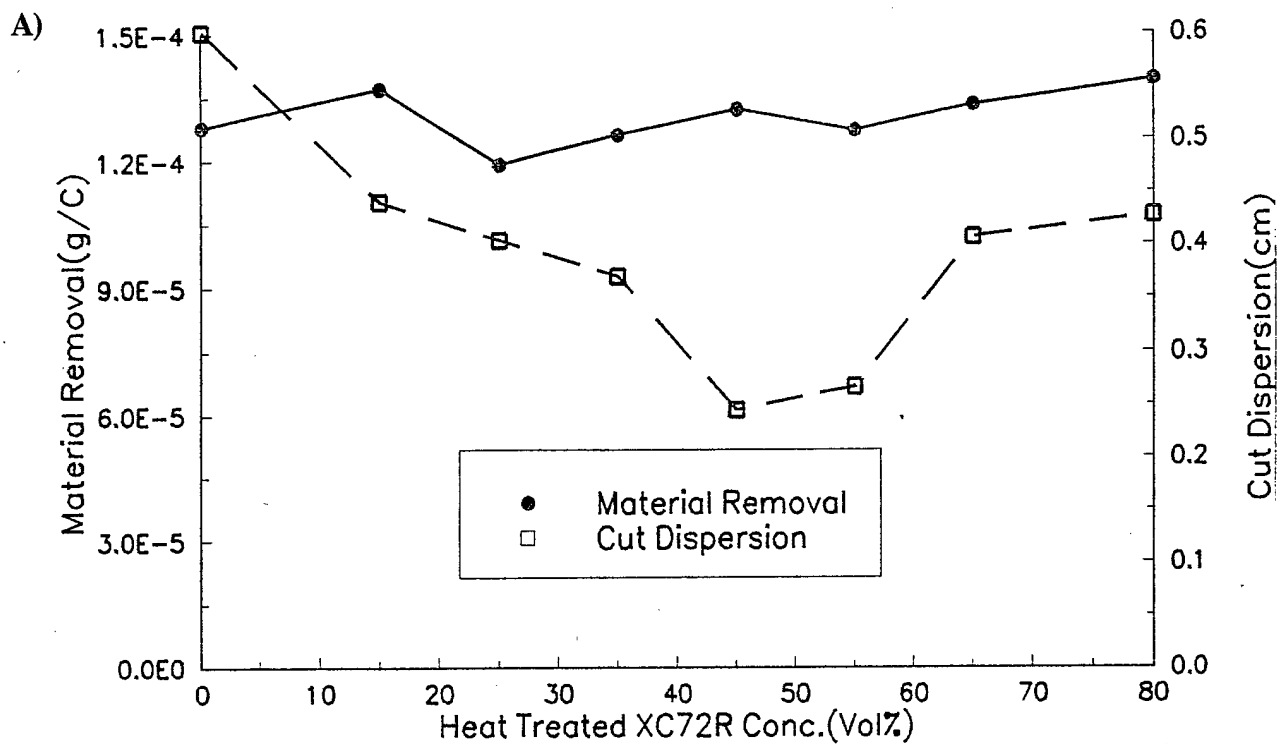


Figure 13. Material removal, cut dispersion, and cell voltage data for the ECM of Ti using heat treated (at 500°C) XC72R particles. Aqueous electrolyte: 3.15M NaBr/1.26M NaNO<sub>3</sub>.

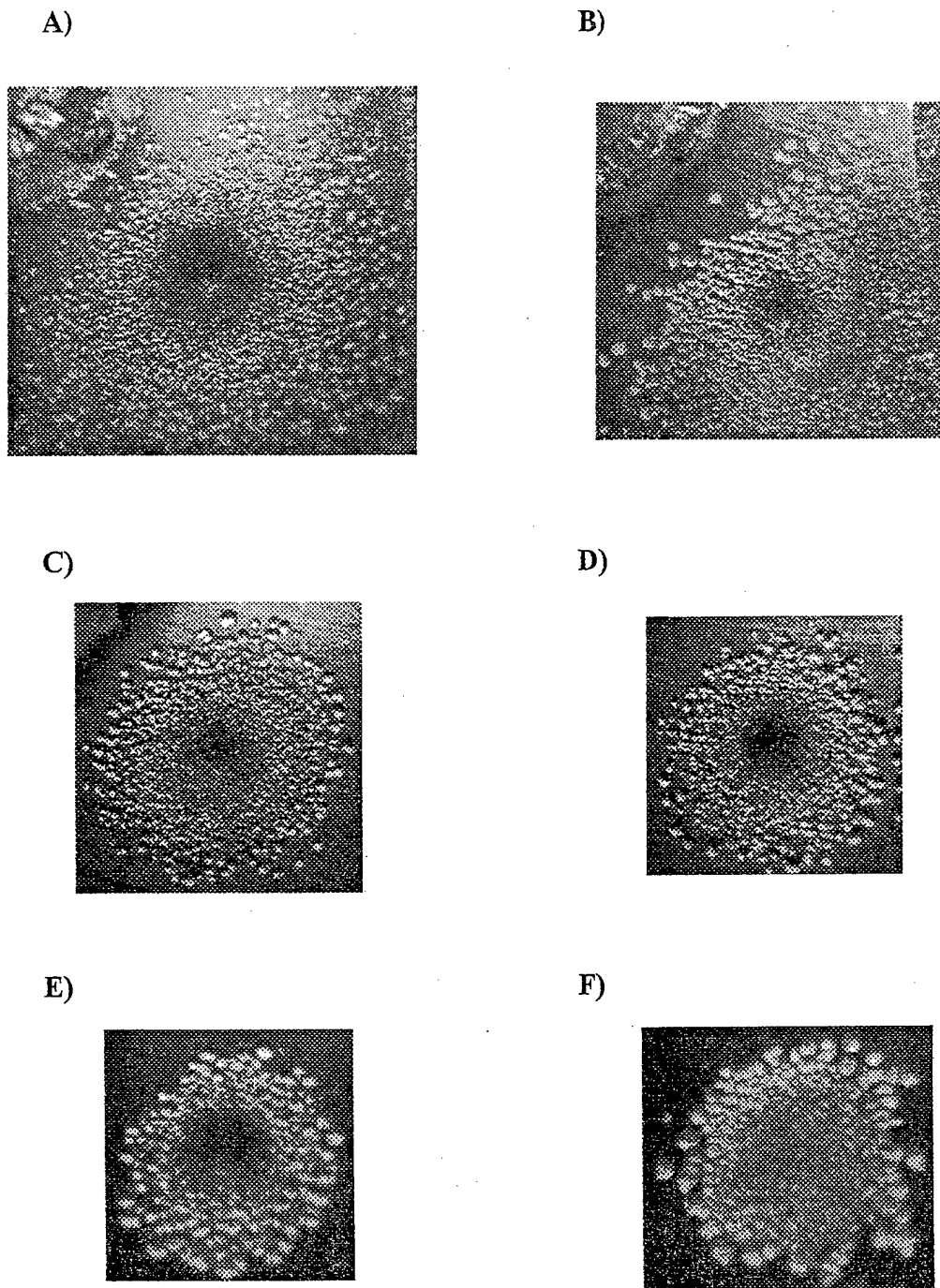


Figure 14. Photographs of Ti coupons subjected to electrodisso- lution in 3.15M NaBr/1.26M NaNO<sub>3</sub> with A) 0%, B) 15%, C) 25%, D) 35%, E) 55%, and F) 65% (by volume) XC72R (heat treated in air at 500°C).

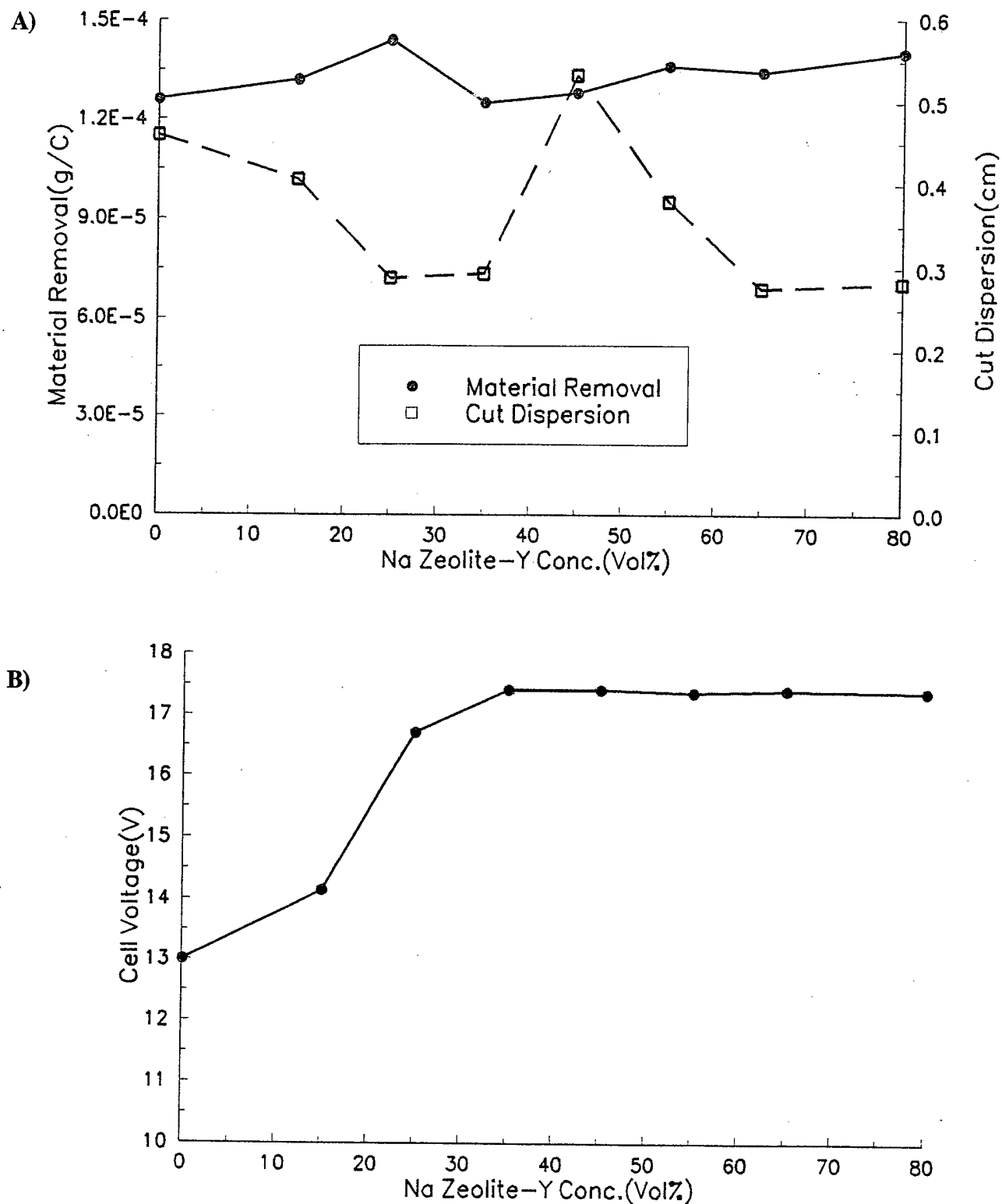


Figure 15. Material removal, cut dispersion, and cell voltage data for the ECM of Ti using Na zeolite-Y particles. Aqueous electrolyte: 3.15M NaBr/1.26M NaNO<sub>3</sub>.

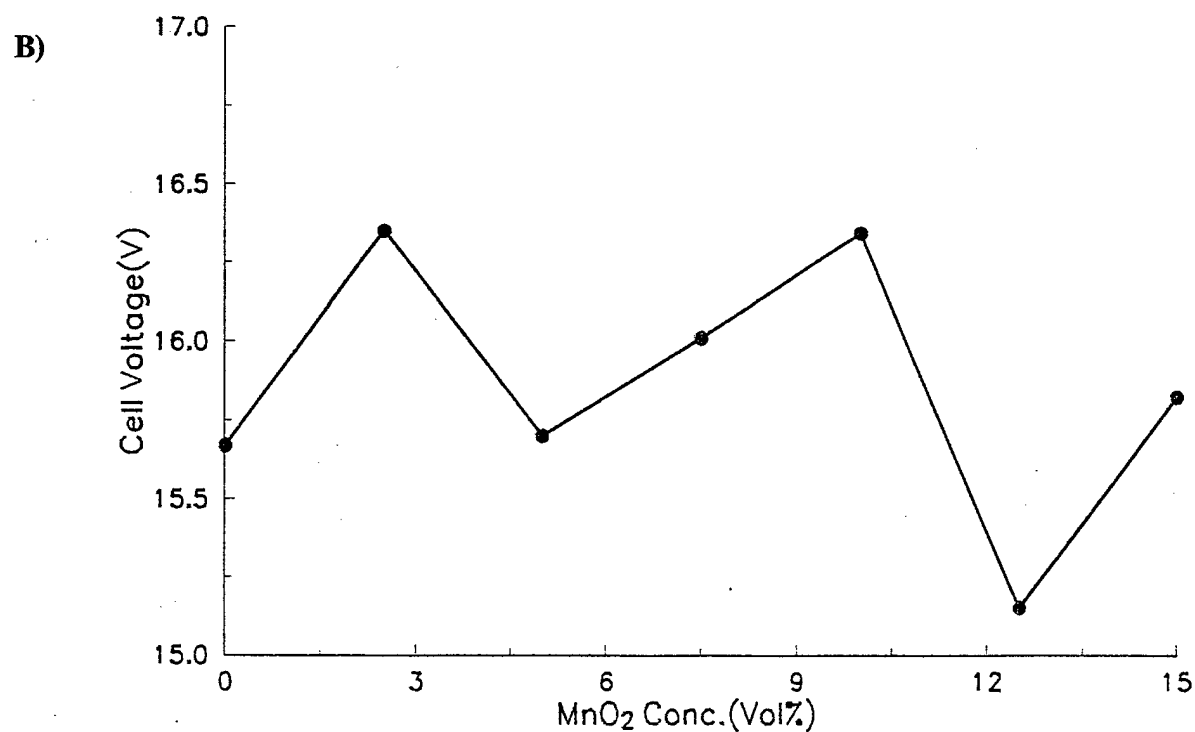
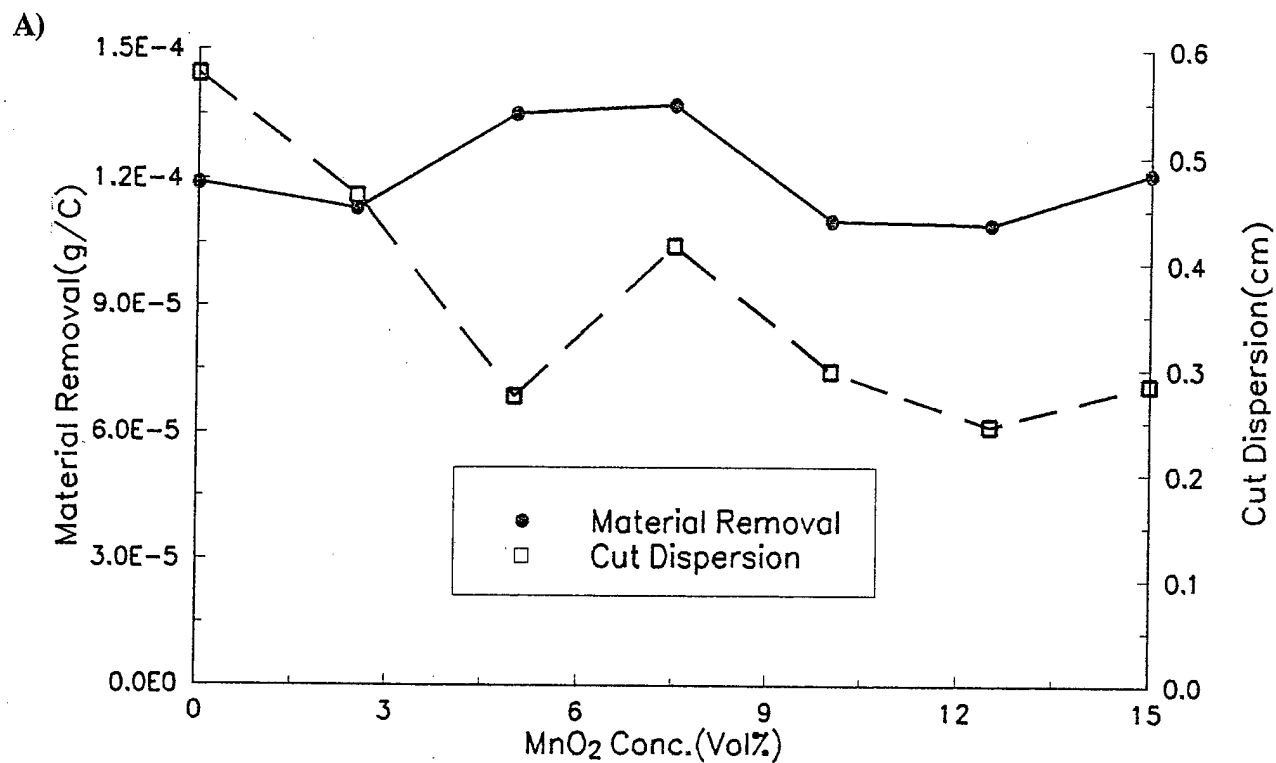


Figure 16. Material removal, cut dispersion, and cell voltage data for the ECM of Ti using MnO<sub>2</sub> particles. Aqueous electrolyte: 3.15M NaBr/1.26M NaNO<sub>3</sub>.



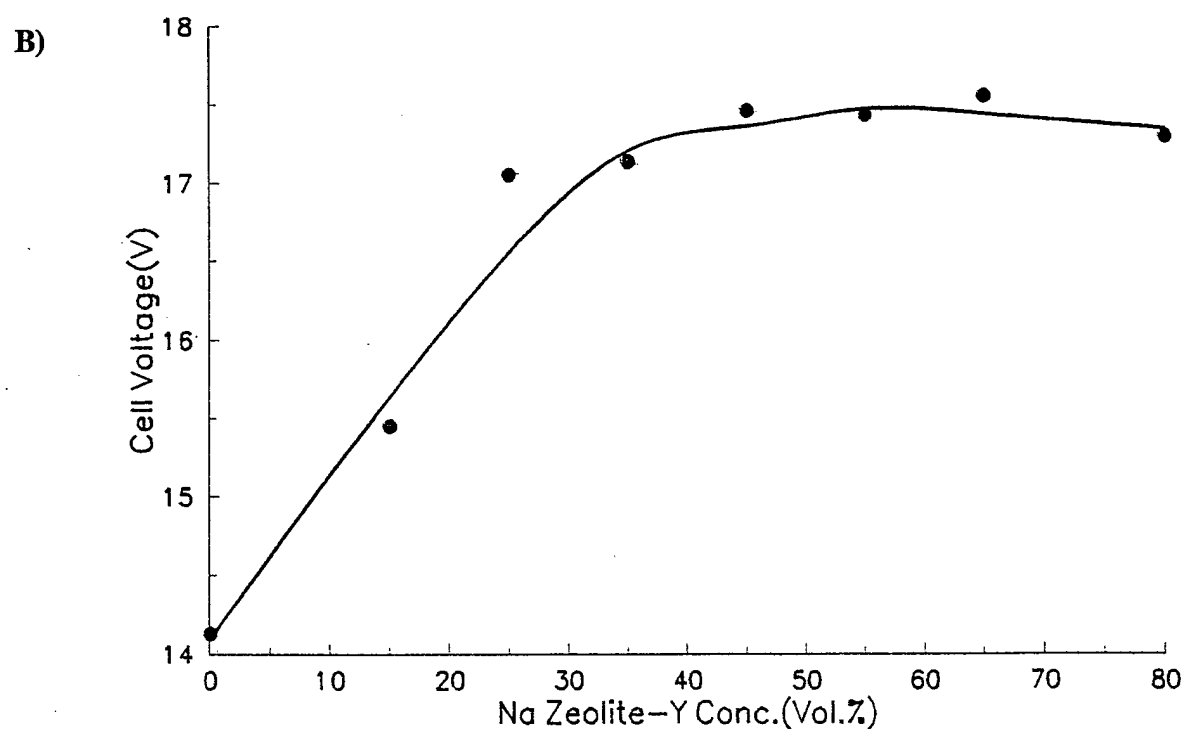
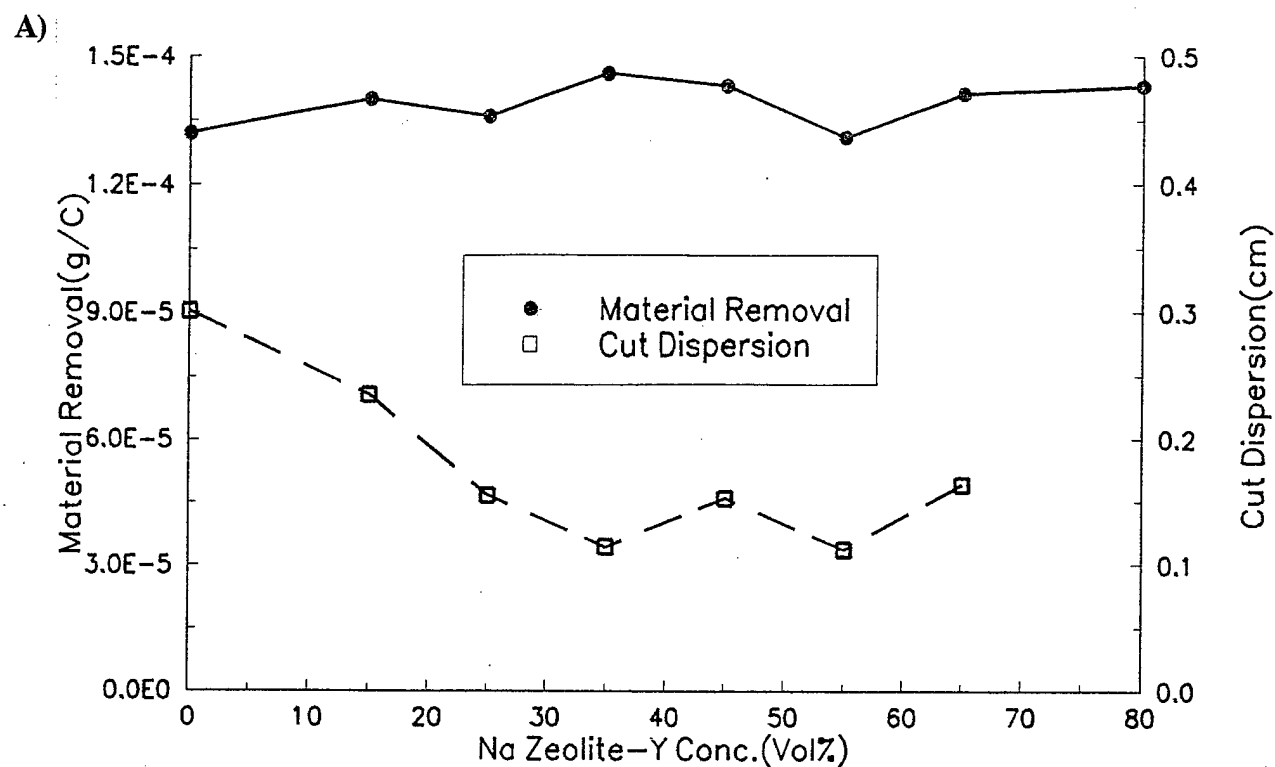
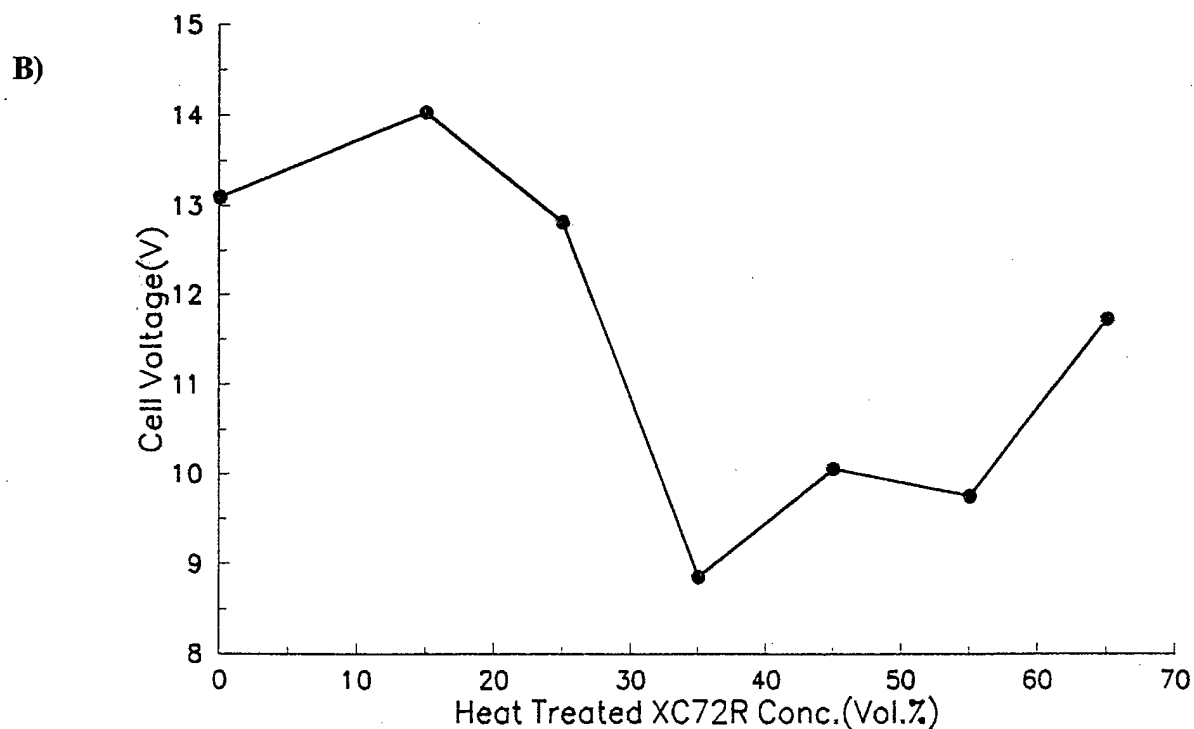
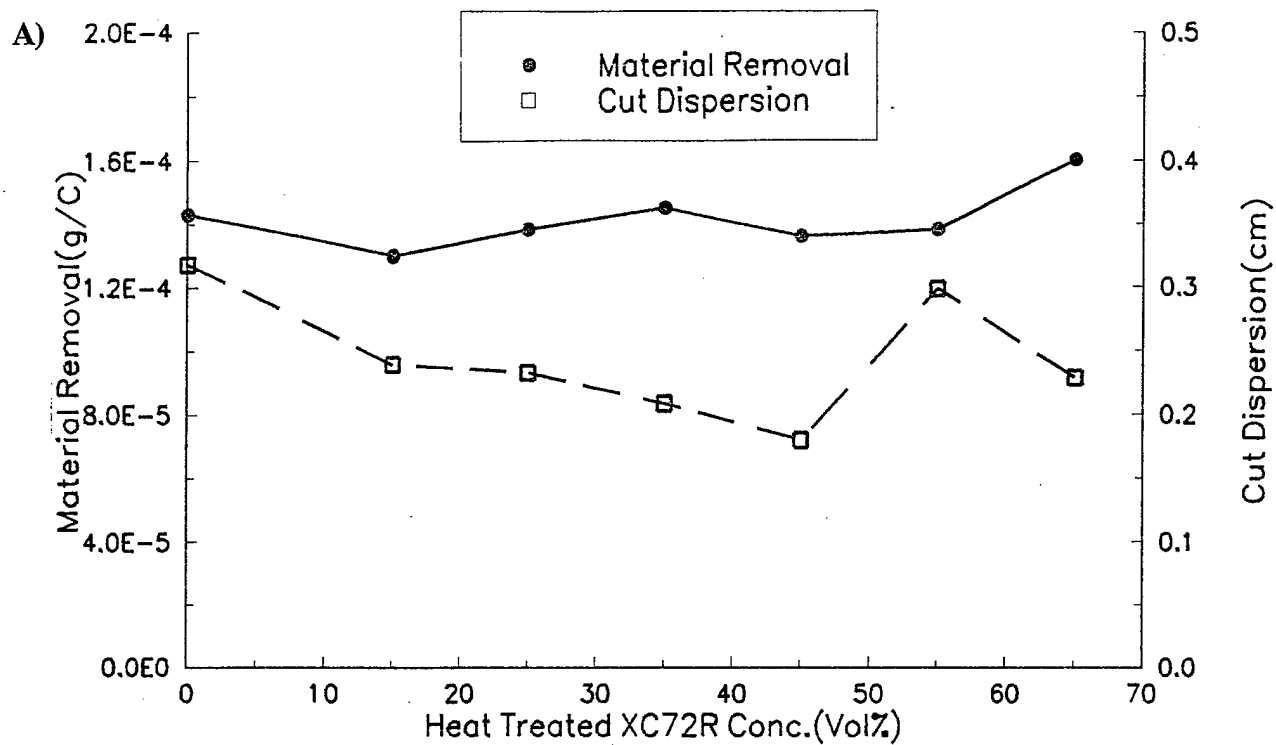


Figure 17. Material removal, cut dispersion, and cell voltage data for the ECM of Ti 6-4 using Na zeolite-Y particles. Aqueous electrolyte: 3.15M NaBr/1.26M NaNO<sub>3</sub>.



**Figure 18.** Material removal, cut dispersion, and cell voltage data for the ECM of Ti 6-4 using heat treated XC72R (at 500°C) particles. Aqueous electrolyte: 3.15M NaBr/1.26M NaNO<sub>3</sub>.

Data for the ECM of Ti 6-4 using untreated XC72R is given in Figure 19. As was the case with heat treated XC72R, untreated carbon produced significant reduction in the operating cell voltage, with a minimum being observed at 45vol% where cut dispersion was at a minimum. Stray pitting was apparently also minimal at this concentration.

The addition of increasing amounts of manganese dioxide to the electrolyte resulted in a gradual increase in cut diffuseness, while the operating voltage was reduced. This data is shown in Figure 20. At 12.5%  $\text{MnO}_2$ , the cut was over a substantial portion of the coupon surface. This is in marked contrast to the cases with XC72R and zeolite, and may be a particle size effect, as the particles in this case were rather coarse.

Using this approach the ECM of Ti 6242 is shown in Figure 21. This data shows a minimum in cut diameter at between 7.5 and 12.5vol%  $\text{MnO}_2$ . Material removal was at its maximum in the absence of particles and at an intermediate particle concentration (10vol%). The overall cell voltage actually increased with concentration of added  $\text{MnO}_2$ . The number of pits diminished with the addition of  $\text{MnO}_2$  above 2.5vol%.

Data relating to the ECM of Ti 6242 using XC72R is presented in Figure 22. Using heat treated Vulcan XC72R, material removal was found to first decrease to a minimum at about 15-25vol% XC72R, followed by a gradual increase. Cut dispersion decreased rapidly with added XC72R, while the final cell voltage increased to a plateau. Pitting was significantly diminished when using the heterogeneous electrolyte compared to homogeneous electrolytes.

Data obtained by ECM using untreated XC72R gave the results presented in Figure 23. A particularly interesting feature is that this data demonstrated dependence on particle concentration, non-monotonic where significant reductions in operating voltage were found at 25% and 60% XC72R. Compared with heat treated XC72R, cell voltage demonstrated a stronger dependence upon cell voltage. The extent of pitting decreased on going from 0 to 25vol% XC72R.

Figure 24 shows data obtained for the ECM of Ti 6242 using Na zeolite-Y. This data showed that decreased cut dispersion occurred, but with more substantial pitting as zeolite concentration was increased. Material removal was quite uniform over the entire particle concentration regime. As expected, the cell voltage increased with increasing zeolite concentration because this dispersant was not an electronic conductor.

Following completion of these designed experiments, the dependence of ECM properties and characteristics on particle type, particle concentration, and alloy composition were examined using the conically tipped graphite electrode under nonflowing electrolyte conditions, as previously shown in Figure 3. This experimental strategy was found to be more effective at determining the effect of current density and field strength on ECM because of a more clearly defined cathode tool shape compared to the ECM lathe.

In summary, titanium metal appeared to be highly susceptible to ECM enhancement by the addition of XC72R particles. Reduced cell voltage, enhanced material removal, cut focusing, and strongly attenuated stray pitting were all obtained with this substrate. Ti 6-4 was similarly effected, while Ti 6242 demonstrated little material removal enhancement and increased cell voltage. These results imply that the addition of the refractory elements Al, Mo, and Zr inhibited the amelioration of pitting and the reduction in cell voltage observed with Ti and Ti 6-4 under these conditions. However, ECM of these materials should be

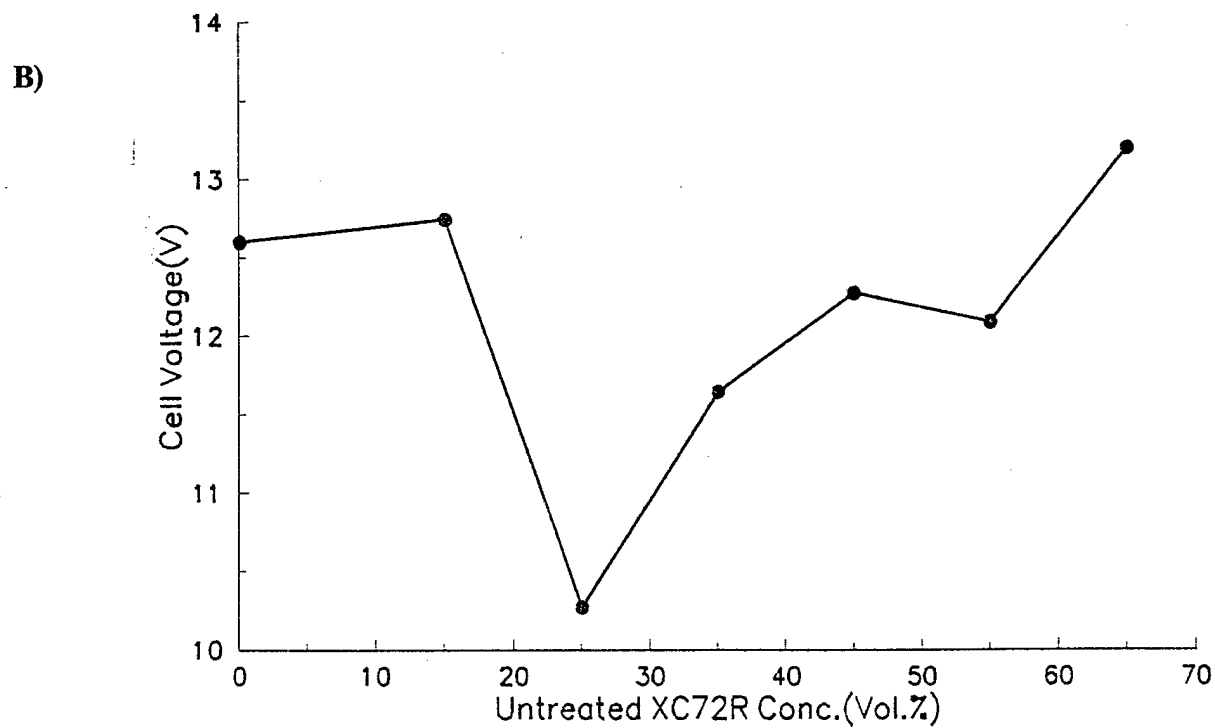
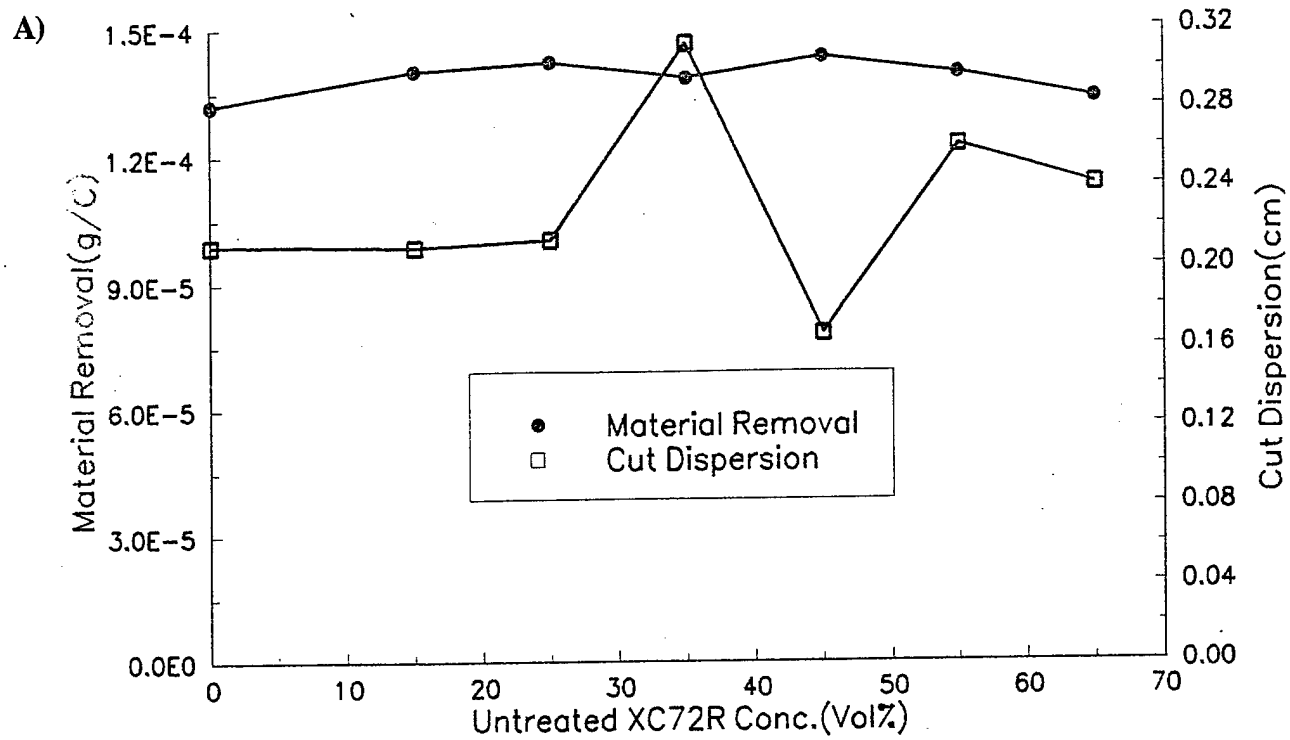


**Figure 19.** Material removal, cut dispersion, and cell voltage data for the ECM of Ti 6-4 using untreated XC72R particles. Aqueous electrolyte: 3.15M NaBr/1.26M NaNO<sub>3</sub>.

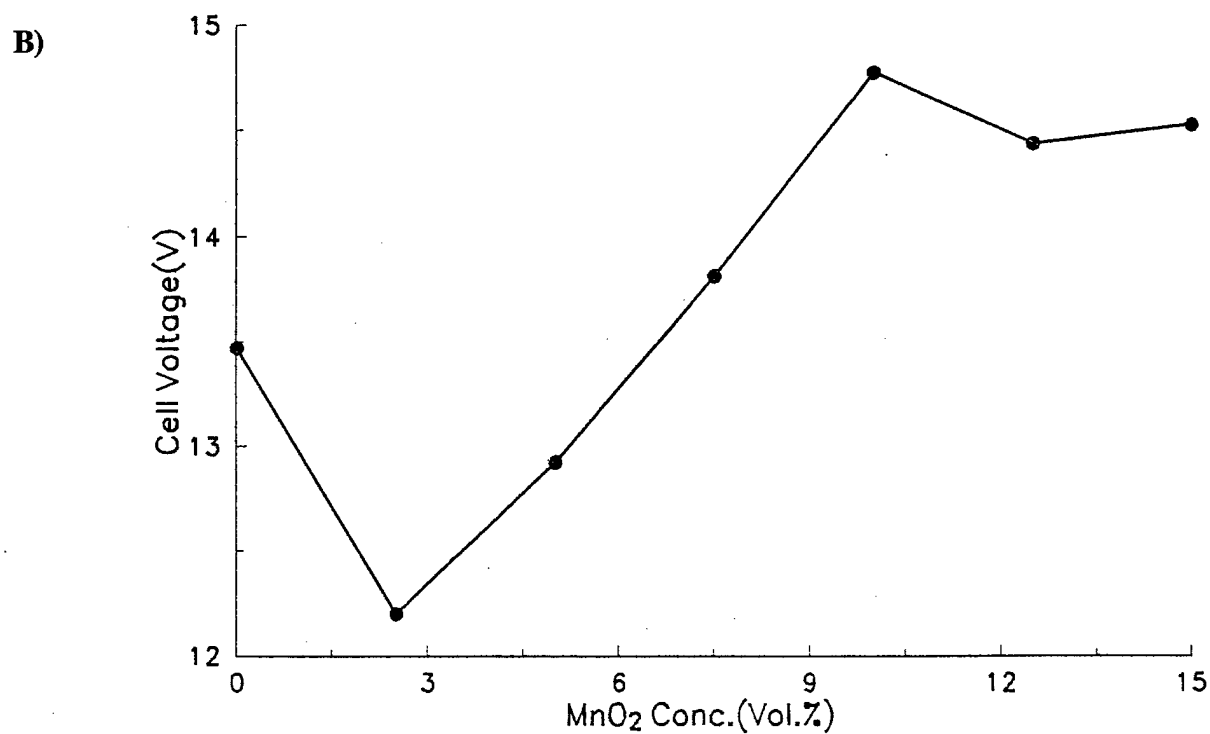
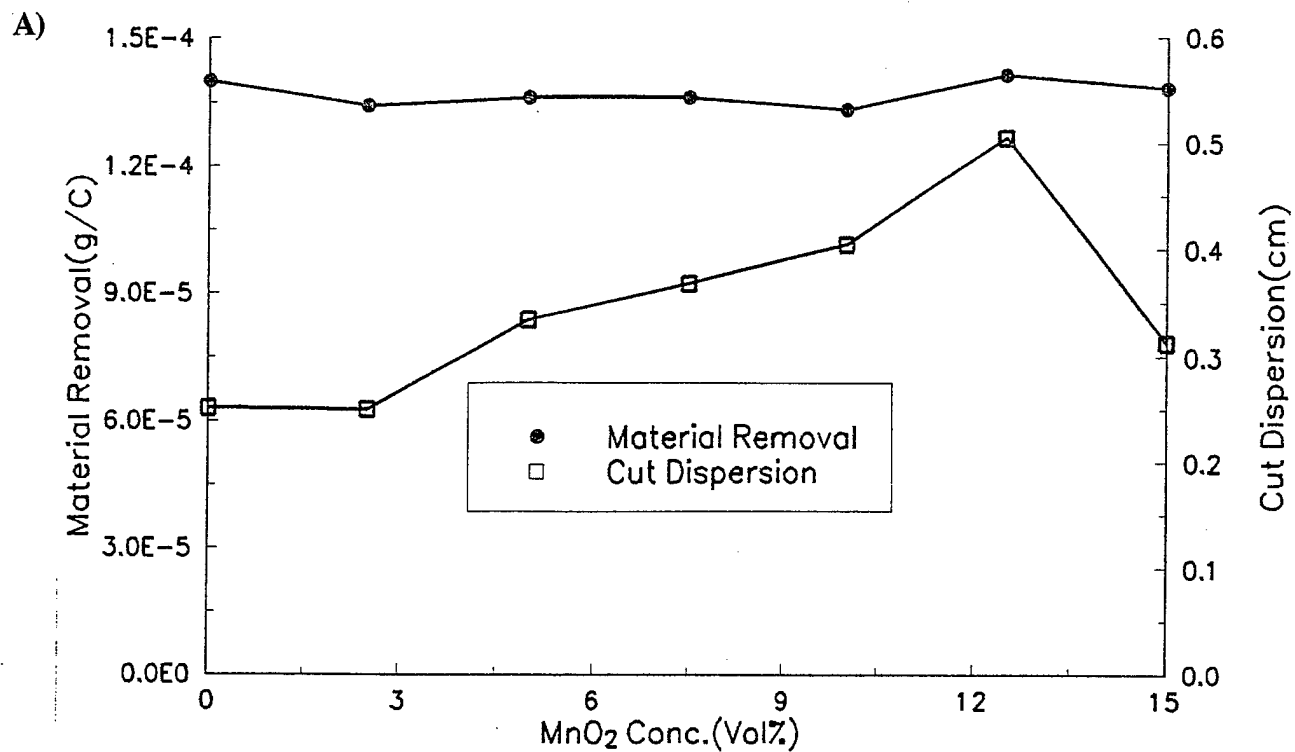


Figure 20. Material removal, cut dispersion, and cell voltage data for the ECM of Ti 6-4 using MnO<sub>2</sub> particles. Aqueous electrolyte: 3.15M NaBr/1.26M NaNO<sub>3</sub>.

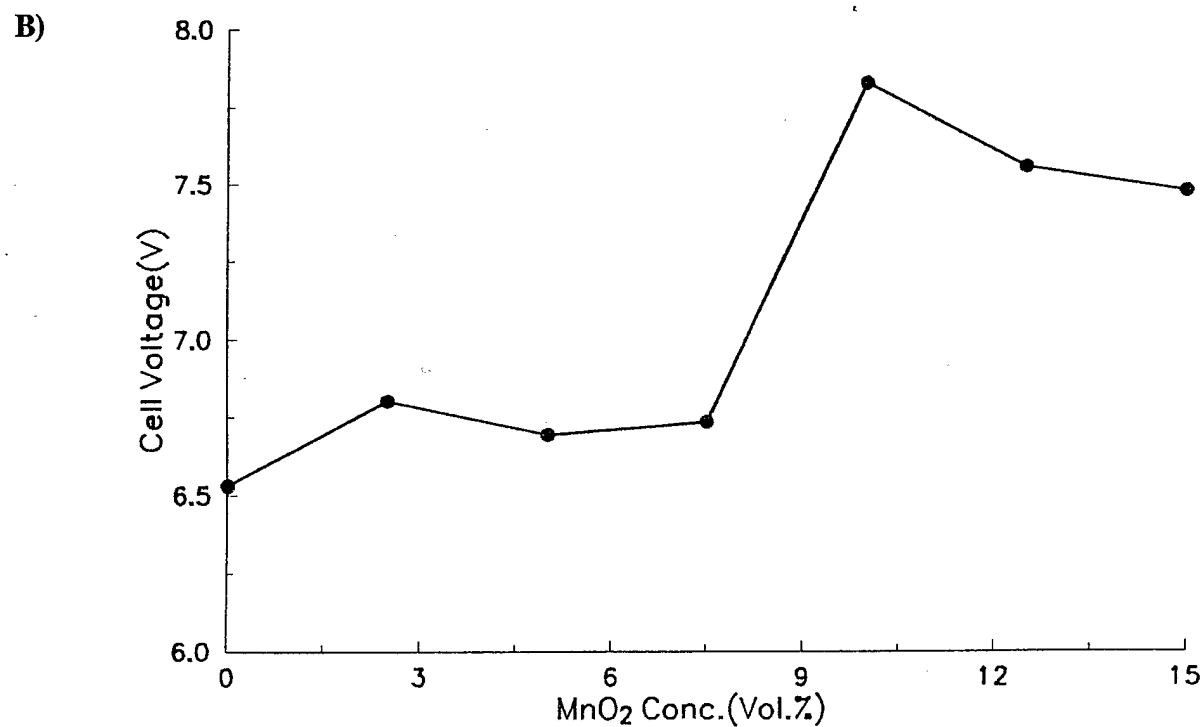
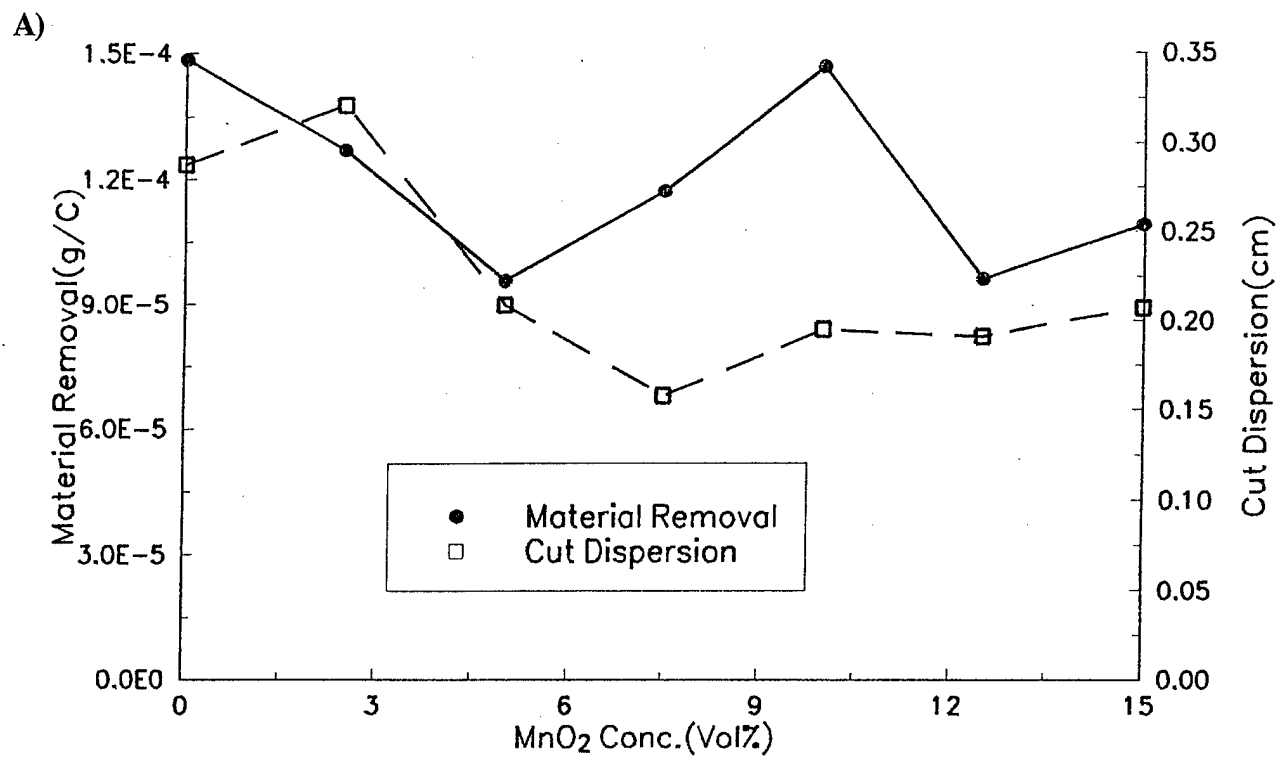
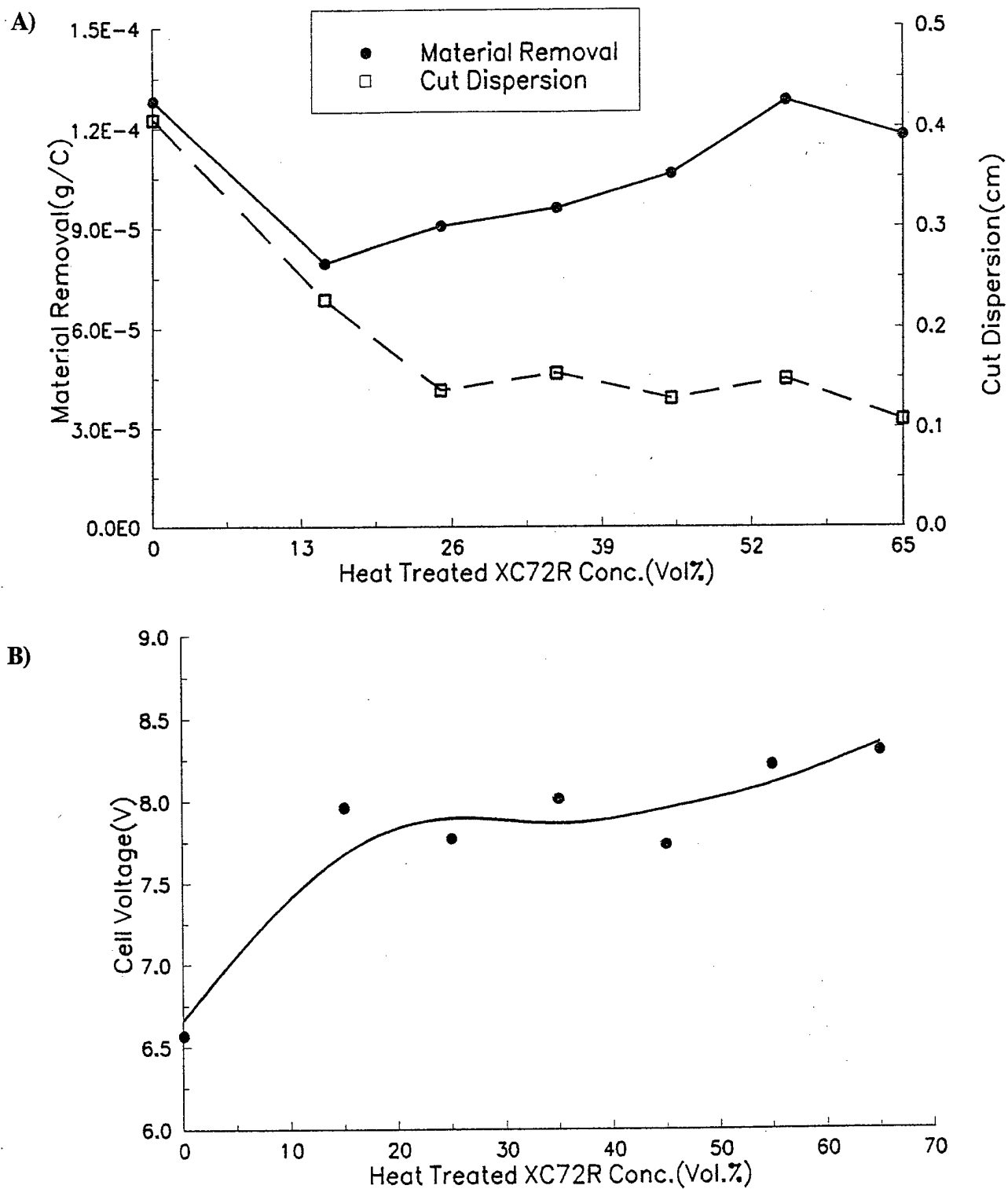


Figure 21. Material removal, cut dispersion, and cell voltage data for the ECM of Ti 6242 using MnO<sub>2</sub> particles. Aqueous electrolyte: 3.15M NaBr/1.26M NaNO<sub>3</sub>.



**Figure 22.** Material removal, cut dispersion, and cell voltage data for the ECM of Ti 6242 using heat treated (at 500°C) XC72R particles. Aqueous electrolyte: 3.15M NaBr/1.26M NaNO<sub>3</sub>.

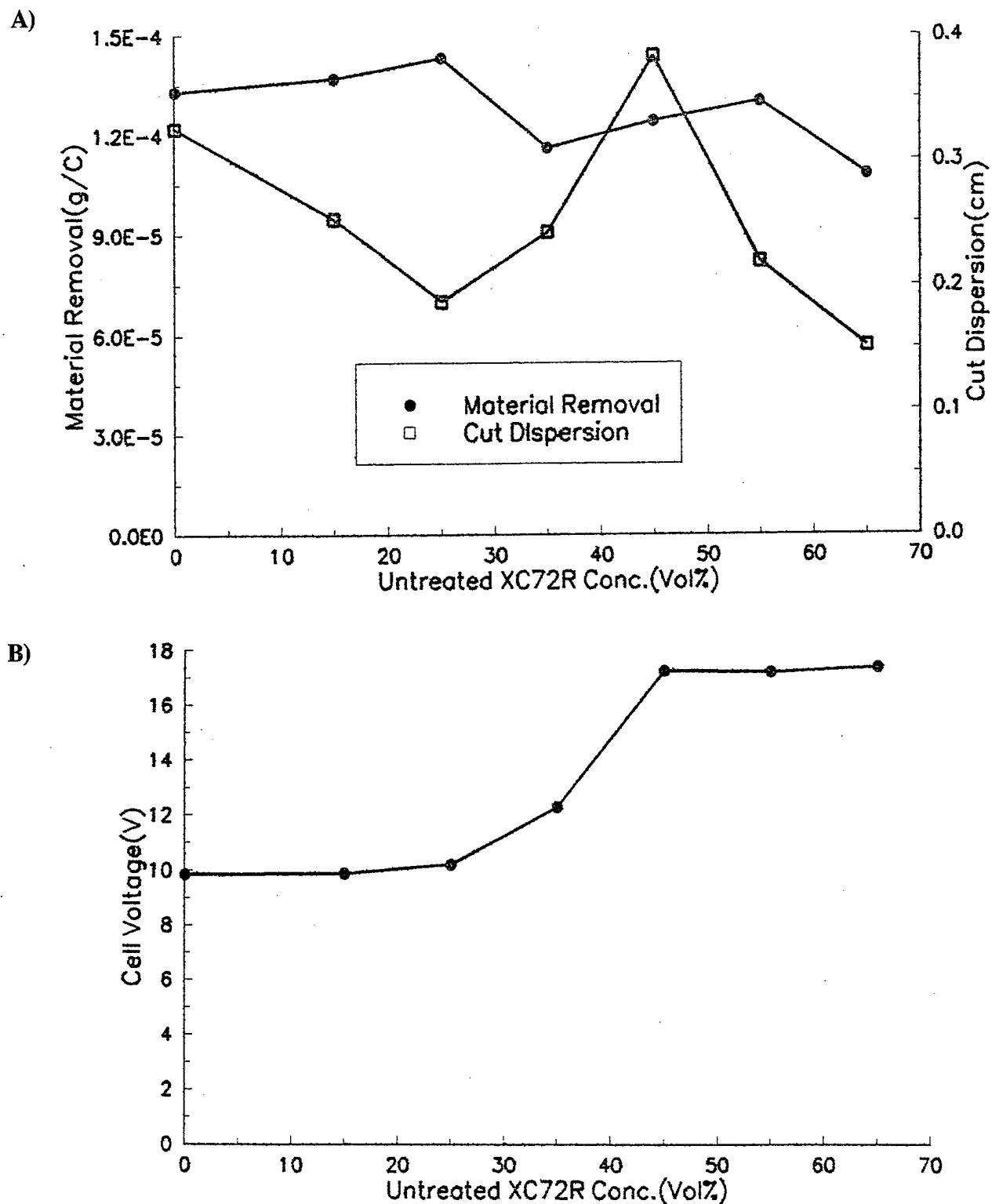


Figure 23. Material removal, cut dispersion, and cell voltage data for the ECM of Ti 6242 using untreated XC72R particles. Aqueous electrolyte: 3.15M NaBr/1.26M NaNO<sub>3</sub>.



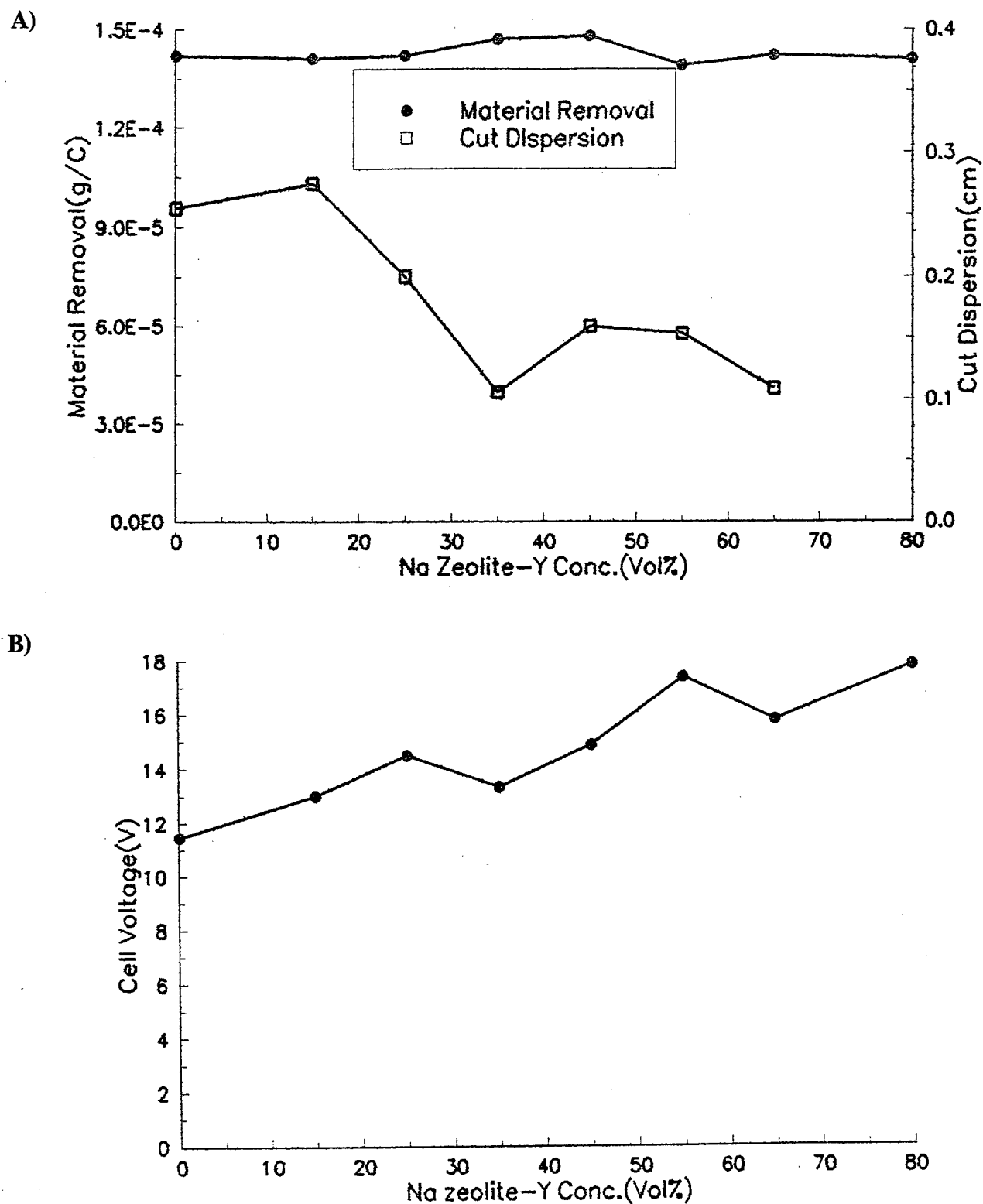


Figure 24. Material removal, cut dispersion, and cell voltage data for the ECM of Ti 6242 using Na zeolite-Y particles. Aqueous electrolyte: 3.15M NaBr/1.26M NaNO<sub>3</sub>.

enhanced by the addition of more aggressive species (such as  $\text{Cl}^-$  or  $\text{F}^-$ ) to the electrolyte. This effect was also observed with the ECM of Ti in NaCl versus NaBr/ $\text{NaNO}_3$  electrolyte: the former gave no stray pitting, while the latter gave extensive pitting.

Experimental data obtained during this task using the prototype ECM lathe and subsequently performed analyses suggested the most important variables for each material and hence, operating conditions to be employed in Task 3. Additionally, determination of most influential variables will help focus the course of proposed work during the Phase II program.

### ***Task 3      Electrochemical Machining of Small Diameter Holes in Titanium Alloy Coupons***

Work performed to this time in the program identified preferred conditions for electrochemically machining selected titanium alloys. These insights were applied on the prototype ECM lathe (Figure 15) for drilling holes in titanium alloy coupons. Preferred conditions for the ECM of titanium alloys were found to invariably utilize carbon particles, and in particular, XC72R heat treated in air. Carbon particle volume concentrations of between 15 and 35% were found to give the best overall performance in terms of material removal enhancement cell voltage reduction, reduced stray pitting and focus cut diameter. Preferred electrolytes were found to be NaBr or NaBr/ $\text{NaNO}_3$ . Smaller anode-cathode gap spacings and a translating cathode produced the best shape resolution and lowest steady cell voltages. Lower current densities favored higher material removal efficiency, but resulted in lower possible feed rates. As the concentrations of metals producing refractory oxides (such as Al, Mo, and Zr) within the titanium alloys were increased, there was less tendency to give reduced cell voltage and pitting with the addition of particles.

As a consequence of the above observations, the following conditions were selected for the drilling holes into Ti alloy coupons: 25vol% XC72R, 3.15M NaBr/1.26M  $\text{NaNO}_3$ , anode-cathode gap of 48 microns, electrolyte flow rate of 7ml/sec, current density of 35A/cm<sup>2</sup>, electrolyte temperature of 25°C, and cathode tool translational speed of 0.002mm/sec were chosen as variables for the drilling of holes into Ti, Ti 6-4, Ti 6242, and  $\text{Ti}_3\text{Al}$  coupons. Holes were drilled into Ti, Ti6-4, Ti6242, and  $\text{Ti}_3\text{Al}$  in 25% XC72R/3.15M NaBr/1.26M  $\text{NaNO}_3$  with other conditions as described in the preceding paragraphs.

Successful completion of this Phase I program resulted in defining the viability of electrochemically machining selected titanium alloys at high rates and with high precision using aqueous electrolytes incorporating dispersed conducting microparticles.

## **IV. SUMMARY OF PHASE I RESULTS**

- Cyclic voltammetry measurements performed in heterogeneous electrolytes confirmed that both voltage reduction and enhanced titanium oxidation currents resulted from the strategy investigated.
- Experiments performed using a solid graphite cathode and selected heterogeneous electrolytes under non-flowing conditions studied showed that, depending on the titanium alloy being subjected to ECM, material removal rate and dimensional

control were dependent upon the type and concentration of particles dispersed within the aqueous electrolyte.

- The electrolytes NaCl, NaBr, NaNO<sub>3</sub>, and NaBr/NaNO<sub>3</sub> mixtures were examined in the absence of particles for each of the titanium alloys studied. NaCl was found to be the most aggressive electrolyte, producing highest material removal rates, but mixtures of NaBr and NaNO<sub>3</sub> were found to give the most effective dimensional control.
- Experiments designed via the Plackett-Burman design approach, and conducted with an ECM lathe showed that virtually all of the variance in ECM results could be accounted for using 10 experimental variables and that: 1) stray pitting was most sensitive to the alloy type, particle type and concentration, and that pitting was reduced by the presence of dispersed particles, 2) material removal and cut shape (depth and diameter) were most sensitive to current density, 3) cell voltage was most sensitive to anode-cathode gap, but was also sensitive to the type and concentration of particles: increasing the concentration of conductive particles tended to lower the overall cell voltage, and 4) cut diameter was sensitive to particle type and concentration. In conclusion, particle type and concentration were found to exhibit significantly favorable contributions to the ECM of titanium alloys. Based on the magnitudes of regression coefficients, cut dispersion and stray pitting were most affected by the inclusion of dispersed particles within the heterogeneous electrolyte.
- Material removal enhancement was highest for pure titanium (25% over particle-free electrolyte) using dispersed XC72R within the heterogeneous electrolyte. Relative rates for ECM material removal using XC72R-containing heterogeneous electrolytes was found to be Ti > Ti6-4 > Ti 6242.
- The dispersion (width of cut) of material removal when an ECM cut was made using a conical (pointed) cathode was found to depend strongly on particle type and concentration, and the nature of the anode material. Dispersion was typically reduced by the addition of particles, with the exception of ECM of Ti6-4 in the presence of MnO<sub>2</sub>.
- Using graphite cathode under nonflowing conditions, propensity towards stray pitting was markedly reduced at intermediate concentrations for all particles studied with the exception of Na zeolite-Y. This effect was most substantial for pure titanium using XC72R heat treated at 500°C. The ability to ameliorate stray pitting decreased in the order XC72R (heat treated) > XC72R (untreated) > MnO<sub>2</sub> > Na-zeolite Y.
- The susceptibility of the materials studied to stray pitting increased in the order Ti < Ti 6-4 < Ti 6242, pointing to the probable role of Zr and Mo in the formation of pits in the latter titanium alloy.

- The techniques of electrochemical hole boring, electrochemical grinding, and electrochemical machining were represented in the application of both preliminary cells and the ECM lathe apparatus.
- A prototype ECM lathe incorporating a stepper motor driven translation stage was implemented during this program. Using this hardware holes were successfully drilled into titanium alloys at higher rates than would be anticipated using conventional ECM technology.

## V. ESTIMATE OF TECHNICAL FEASIBILITY

The phenomena investigated here will eventually, in Phase III, lead to a commercial process incorporating preferred heterogeneous electrolytes, and operating conditions for the ECM of titanium and selected titanium alloys used in Navy aircraft engines. We anticipate that this will lead to production level machinery possessing the general design shown in Figure 25 for the processing of turbine components. The ECM machine will consist of multiple cathodes each of which possess translational (for linear feed) and rotational (for curvature of surfaces) degrees of freedom. The workpiece (anode) - a blisk - will be mounted on a hub in the center of the machine. The heterogeneous electrolyte will be delivered via flow channels in the cathode towards the anode workpiece. Spent electrolyte will be collected in a reservoir at the base of this experimental assembly. A large (up to 30,000A) power supply will be used to provide a voltage or current source for machining.

The machine described above will be incorporated into a closed loop system as shown in Figure 26. Spent heterogeneous electrolyte slurries will be filtered, with reintroduction of filtered electrolyte. After several cycles, the electrolyte may be spent or found such that it may have to be replaced. In this event, a fresh electrolyte vessel will be in place. Filtered solid will be transferred to a mixing chamber along with the electrolyte filtrate, and the slurry reconstituted.

Technology features making this approach attractive for commercialization include i) a lower required operating voltage ii) control over the lateral extent of cuts, iii) enhanced material removal rates, and iv) the ability to focus cuts for enhancing machining precision.

Phase I results demonstrated cell voltage reductions of the order of a factor of 1.5 (with Ti). Material removal enhancements of up to 50% (with Ti) were also obtained. Also, cuts focused up to a factor of 4 were realized (with Ti and Ti 6242). The use of these results in predicting potential improvements can be presented here. From these results estimates can be made an anticipated operating cost improvements by applying technology identified during performance of Phase I program. For example, with the titanium alloy studied here, a decrease in operating cell voltage of from 13V to 7.5V was obtained at a current of 1A with an anode-cathode gap spacing of 0.82mm. Typical full size industrial ECM equipment operates at 30,000A (about 100A/cm<sup>2</sup>). For a typical operating voltage of 14V, addition of an electronic conducting dispersion into the aqueous electrolyte we project would lower the operating voltage of 4V. This represents, for a maximal linear machining rate of 0.9cm/min and a turbine blade length of 15cm, about 16-17min. for rough cutting each blade. For a turbine with 80 of these airfoils, 1330min will be required for machining of each blisk. This

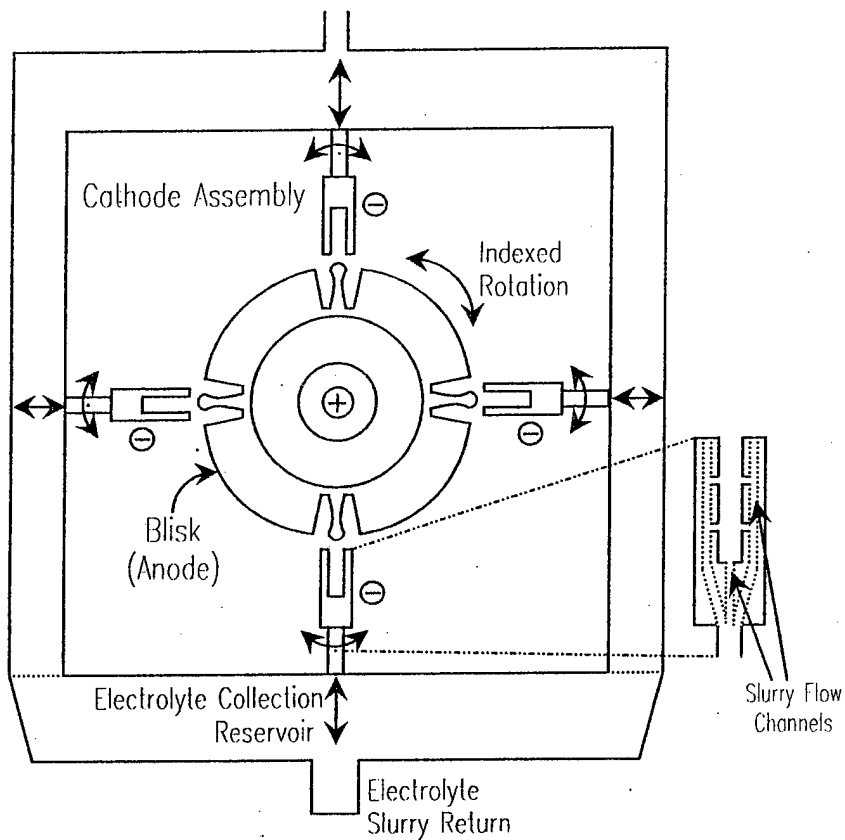


**Figure 25.** Schematic of production hardware to evolve in the course of this program for the ECM of titanium alloys into turbine blisks for Navy aircraft.

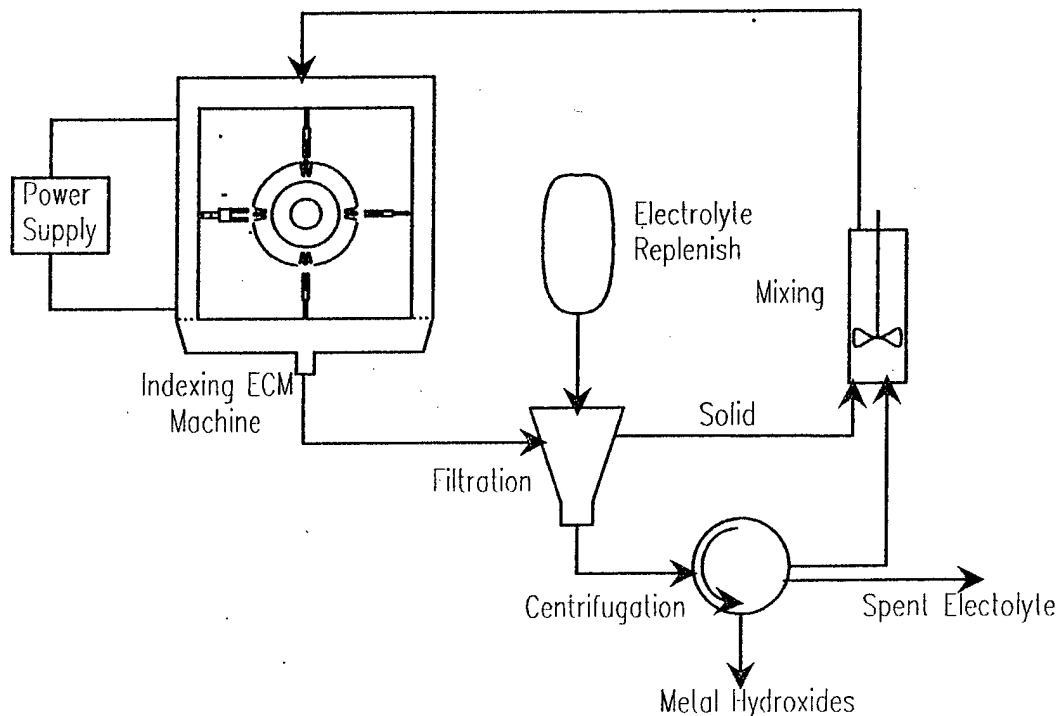


**Figure 26.** Schematic of overall process for the processing and recycling of heterogeneous electrolytes used in the ECM of titanium alloys.

corresponds to 9330kWh per blisk or, at a cost of \$0.05/kW-h, about \$470/blisk. For throughput of 25 blisks/week, a total savings of \$12,000/week could be anticipated from energy savings alone. However, another very profound effect would be obtained: an improvement in dimensional tolerance due to the constancy of the cell voltage arising from the persistent conductivity made and resulting in ameliorated Joule heating.

## **VI. TOWARDS COMMERCIALIZATION**

### **A) Commercial Applications**

This technology will find application for the precision ECM of titanium alloy components of interest to engine components in Navy aircraft. A particular feature of this technology is its applicability to the machining of complex shapes in the absence of stray pitting with high precision under significantly lower power requirements than conventional ECM technology. Enhanced machining precision is also facilitated by lower electrolyte Joule heating.

In addition to the application of these heterogeneous media to ECM, this technology will find application in i) tools possessing the ability to achieve cut dimensional control, ii) electrorheological fluids possessing continuously adjustable viscous properties by application of an electric field, iii) measurement of fluid transport properties from detected current-voltage characteristics, and iv) nanotechnology machining applications.

The application of dispersed particulates in dielectric media as "smart" fluids would be a potentially very broad and profitable market. Such media, incorporated into appropriate devices, would find application in electric field controllable shock absorbing, vibration damping, mechanical power transmission, selective lubrication, flow control, "smart" sealing of leaks, information processing and storage (by means of the capability of forming information-containing clusters and fibrous structures of various sizes and shapes), nano- and micromachining, electric field control of transport processes in liquid phase chemical reactions, and control of chemical species permeation rates through polymer membranes as would be necessary in ameliorating the methanol crossover problem in direct methanol fuel cells.

As a consequence technology to emerge in this program would also have broad commercial applications beyond ECM.

### **B) Patent Status**

A U.S. Patent application on this ECM approach has been filed (August 29, 1995) entitled, "Machining by Electrical Removal of Materials Utilizing Dispersions of Insoluble Particles", inventor J.H. White, Docket number V95PERI-7.

### **C) Uniqueness of the Technology Approach**

The uniqueness of this approach lies in the application of heterogeneous electrolytes to the ECM of titanium alloys. This technology recognizes interrelationships between ECM

cut dispersion, power consumption and Joule heating in the vicinity of the anode workpiece. Furthermore the subject heterogeneous particles are applicable to nonpolar fluids where they can introduce ionic and electronic conductivity, even in the absence of nominally ionic conducting electrolyte.

The approach leads to pit-free machining. Another feature of this approach is that the electric field applied across the heterogeneous fluid will impose electrorheological effects whereby dispersed particles become ordered into fibers or clusters thereby modifying fluid transport properties locally within the anode - cathode gap region. This effect facilitates achieving greater control over ECM cut tolerances than with conventional ECM.

## **D) Markets**

Potential impact of the subject ECM technology can be estimated by considering the reduced time required to machine a blank titanium alloy component into an integrally bladed rotor (IBR) used in Navy jet engines. Using conventional machining techniques, 1000hrs of machining time are required to produce a finished IBR. Based on experimental performance found to this time in the program ECM time would be reduced to 50 hours. Further value added would be obtained as a consequence of reduced stray pitting and resulting improved machining tolerance.

A significant market for ECM hardware currently exists. The world market for ECM equipment was valued at \$90.5 million in 1992, while the U.S. market was \$23.4 million. Both markets are predicted to grow at 6.1-6.3% per year through 1999 with the world market expected to reach \$137 million and the U.S. market to \$35.9 million by 1999. Worldwide, 259 ECM units were sold in 1992 with this predicted to rise 466 units by 1999. The average unit price in 1992 was \$350,000. Technology being developed in this program will be directed towards cooperative agreements with companies already engaged in production level ECM. Since ECM is practiced by a relatively small number of companies, it is anticipated that a sizeable share (up to 30%) of the market engaged in ECM can be captured within five years after implementation.

## **E) Anticipated Competition**

There are potentially competitors in both the hardware and process ends of the ECM market. Major ECM hardware vendors worldwide include Anocut with a 24.6% market share, Surf/Tran (18.9%), Extrude Hone (16.6%), and Chemtool/Dynetics (9.6%). Major end users for ECM equipment include aerospace and defense industries, the automotive industry, and industrial/electrical machinery and equipment companies. The process will potentially impact these hardware manufacturers, since new modalities for carrying out ECM and methods of measurement can be anticipated to be developed, leading to new hardware implementations. However, as previously indicated. Among potential competitors are Lehr Precision, Inc., GE Aircraft Engines (GE), and Pratt and Whitney (PW). It should be realized that, in the aforementioned industries, processing via ECM is often done by a smaller contracting company. This relationship is illustrated by consideration of that between Lehr Precision Inc. and respectively GE and PW. In such a situation our competition will

not be the larger entity but the smaller manufacturing company lacking R&D and product development functions dedicated to ECM. Consequently, commercialization could be looked upon as being initiated with the Phase II effort and ending, after completion of Phase III, with an implementable process.

#### **F) Competitive Advantages**

The potential economic advantages of this ECM technology have been previously discussed in this document for the fabrication of Navy aircraft engine components and resulted in significant energy savings. In addition to this for an 88 or 89 blade rotor, the cost of pitting in terms of machining time we expect would be substantial: the operations in the above paragraphs comprise less than 50% of the total machining time. The remainder is taken up in the finish stages. Although at this point, the feed rate is 2-3 times that during the rough cutting stage, the finish cut requires roughly half of the total machining time, due essentially to the need to slave, deslave, and reslave turbine blades outside of the cut region. Eliminating the occurrence of stray pitting and the resultant need for the reslave/deslave cycles could potentially reduce time and costs by about 25-30%.

The economic benefits to be obtained by employment of the approach can be summarized:

- Effectively extending the cathode into close proximity to the titanium alloy workpiece, thereby dramatically lowering the necessary ECM operating voltage by reducing interelectrode resistance.
- Improving shape resolution of the ECM process by the aforementioned extension of the cathode into the immediate anode vicinity.
- Improving dimensional control of components subjected to ECM by reducing Joule heating.
- Facilitating enhanced material removal rates during the ECM of titanium alloys.
- Ameliorating stray pitting by the elimination of strongly complexing anions from solution and their replacement with massive framework anions.

#### **G) Towards Commercial Production**

As we see it at this time implementation of this technology on the commercial scale will be achieved by incorporating the process into currently existing ECM hardware suitably modified to accommodate our approach. This will be achieved by formalizing a business relationship with a company in the Denver area possessing ECM production capacity. Financing for this joint business initiative will come from Venture Capital Investment. We anticipate that a separate company, jointly owned by these three parties will be formed, for the express purpose of developing and implementation of this technology.



The production plan leading to development of ECM hardware, will proceed in the following stages:

- Adapt optimized process operating conditions identified during performance of the overall program, incorporating preferred heterogeneous electrolytes, into production ECM hardware.
- From ECM performance on titanium alloys using production scale hardware, an all-purpose, full-scale engineering ECM prototype possessing the desired attributes necessary for production level work will be designed and fabricated.
- Using engineering ECM hardware preferred operating parameters will be selected for the machining of candidate titanium alloy substrates.
- Using the data obtained from the engineering prototype, design and fabricate equipment, including auxiliary equipment, necessary for the processing of production components.
- Using information derived from operation of the production prototype, develop a set of procedures for the ECM of typical components.
- Develop appropriate quality control (QC) procedures for parts electrochemically machined using this technology.
- Perform production runs to confirm whether design and QC procedures are compatible with specifications of finished components.
- Incorporate hardware into production plant for component fabrication.

## **H) Marketing Plan**

The business opportunity to emerge will be in providing an ECM service to customers requiring the machining of complex shapes on titanium alloy components.

Steps to be followed towards commercializing research results will be:

- A separate company, jointly owned by Eltron Research, Inc., will be formed directed towards providing ECM service for the processing of titanium alloy components.
- The business relationship between Eltron Research, Inc. and the proposed joint venture will simultaneously be negotiated with the above.
- Perform a thorough market study to identify and assess the markets where application of this ECM service technology will most readily find commercial acceptance in the

near term.

- A comprehensive business and financial plan will be developed, focused on the identified market.
- Appropriate brochures and publicity will be initiated towards making this ECM capability known to those currently requiring such services for the machining of refractory components.

## VII. REFERENCES

1. J.A. McGeough and M.B. Barker, Chemtech, 537(1991).
2. J.A. McGeough, "Principles of Electrochemical Machining", Chapman and Hall, London, 1974.
3. J.A. McGeough, "Advanced Methods of Machining", Chapman and Hall, London, 1988.
4. "Electrochemical Machining", A.E. De Barr, D.A. Oliver, Eds., McDonald, London, 1968.
5. J.F. Wilson, "Theory and Practice of Electrochemical Machining", John Wiley and Sons, London, 1971.
6. J.L. Bettner in "HITEMP Review 1990", NASA Conference Publication 10051, NASA Scientific and technical Information Division, 1990.
7. M. Fleischmann, J. Ghoroghohian, and S. Pons, J. Phys. Chem., 89, 5530 (1985).
8. M. Fleischmann, J. Ghoroghohian, and S. Pons, J. Phys. Chem., 90, 6392 (1986).
9. L.J. Rhoades, U.S. Patent 5,114,548, (1990).
10. F. R. Joslin, U.S. Patent 4,522,692, (1983).
11. M. Fleischmann, J. Ghoroghohian, and S. Pons, J. Phys. Chem., 89, 5530 (1985).
12. M. Fleischmann, J. Ghoroghohian, and S. Pons, J. Phys. Chem., 90, 6392 (1986).
13. D.R. Rolison, E.A. Hays, W.E. Rudzinski, J. Phys. Chem., 93, 5524 (1989).
14. D.R. Rolison, Chem. Rev., 90, 867 (1990).
15. J. Wang, N. Naser, L. Agnes, H. Wu, and L. Chen, Anal. Chem., 64, 1285, (1992).
16. F. Scholz and B. Meyer, Chem. Soc. Rev., 23, 341, (1994).
17. E. Ahlberg and J. Asbjornsson, Hydrometallurgy, 36, 19, (1994).
18. E. Ahlberg and Asbjornsson, Hydrometallurgy, 34, 171, (1994).
19. P.R. Nelson in "Handbook of Statistical Methods for Engineers and Scientists," H.M. Wadsworth (ed.), McGraw-Hill, New York, p. 14.82 (1990).